Strategic Asset Allocation under Narrow Framing / Loss Aversion and Volatility Feedback

Ching-Fan Chung[1]
Institute of Economics
Academia Sinica

and

Chung-Ying Yeh
Department of Finance
National Taiwan University

August 2005

Abstract

We study the dynamic asset allocation problem in a general framework where the representative investor's preferences include narrow framing/loss aversion parameters while the intertemporal budget constraint contains the empirically validated volatility feedback effects. The main conclusion is that the optimal dynamic allocation of wealth among investment, consumption, and savings over different time horizons can be solved in an analytically tractable way and is found to be profoundly influenced by the interactions between narrow framing/loss aversion and the volatility feedback effects. In other words, a more thorough deliberation of the intertemporal budget constraint is indispensable to the analysis of narrow framing/loss aversion preferences in a dynamic asset allocation problem.

Key words: dynamic asset allocation, narrow framing/loss aversion, volatility feedback

---

[1]Corresponding author: Ching-Fan Chung, Institute of Economics, Academia Sinica, Nankang, Taipei, Taiwan. Tel: (886-2) 2782-2791 ext. 188, Fax: (886-2) 2653-3593, E-Mail: cfchung@econ.sinica.edu.tw. We would like to thank Andrew Lo and Jin-Chuan Duan for their helpful comments. The usual disclaimer applies.

1 Introduction

When an investor makes her dynamic decisions about consumption, investment, and savings, the objective is to maximize the lifetime utility generated from consumption. Two features of this framework stand out. First, we note that investment and savings do not enter into the utility function directly and it is consumption that generates utility. Second, investment and savings matter only in terms of theirs contribution to consumption and no distinction is made about how their returns are obtained. Unsatisfied with this simple framework, researchers have proposed the two concepts of narrow framing and loss aversion and offered abundant supporting evidence through experiments on decision-making under risk. If an investor evaluates investment in isolation so that the gain and loss from investment do go into her utility function directly, then we say this investor frames investment narrowly. Moreover, if the investor is more sensitive to losses than to gains from investment in the sense that utility increase resulted from one unit of gain is smaller than utility reduction suffered from one unit of loss, then we say this investor is loss averse (over the investment payoff). Loss aversion is the key component of Kahneman and Tversky's (1979) prospect theory and is found to be supported convincingly by experimental evidence (Tversky and Kahneman, 1991). The effects of loss aversion on financial analysis have been examined by many researchers such as Thaler (1980), Benartzi and Thaler (1995), Thaler, Tversky, Kahneman, and Schwartz (1997), Barberis, Huang, and Santos (2001), to name a few. In particular, many of these authors argued that loss aversion explain the equity premium puzzle; i.e., the puzzling fact that considerably many households do not invest in stocks, which is contradictory to what the conventional asset allocation theory suggests given the historically large equity premium (see, for example, Mankiw and Zeldes, 1991, Mehra and Prescott, 2003). Narrow framing is usually combined with loss aversion to analyze the decision on gambling as have been suggested by Kahneman and Lovallo (1993), Thaler, Tversky, Kahneman, and Schwartz (1997), Benartzi and Thaler (1999), Read, Loewenstein, and Rabin (1999).

As suggested by Barberis, Huang, and Santos (2001), Barberis and Huang (2003), Barberis, Huang, and Thaler (2003), Shumway (1997), Berkelaar, Kouwenberg, and Post (2004), Gomes (2005), exploring how an investor makes the dynamic asset allocation decision under narrow framing/loss aversion can be a useful extension to the portfolio choice literature. In this paper we show that, in contrast to Barberis, Huang, and Santos (2001) and Barberis and Huang's (2001, 2003, 2004) discrete-time models, we are able to divide the optimal investment decisions into the myopic and intertemporal components (of which the former is independent of any future changes in the investment opportunities while the latter is not) and separately examine the short-term and long-term effects of narrow framing/loss aversion in a more general continuous-time framework. More specifically, given that the specification for narrow framing/loss aversion in the utility function is piecewise linear and that the riskfree rate of return is assumed to be a fixed reference point, then the amount an investor will invest in the short-term is more (less) than what can be accounted for by market compensation for risks if the odds of earning excess return from investing a risky asset is larger (less) than the degree of loss aversion. In contrast to this rather natural result with respect to the myopic effects of narrow framing/loss aversion on asset allocation, the intertemporal effects are more complicated and require knowledge about the intertemporal budge constraint that depends on the return process of the underlying risky asset.

To better understand the long term effects, we then propose a flexible diffusion model for risky asset returns that extends Campbell and Hentschel's (1992) discrete-time volatility feedback model which constitutes the second contribution of this paper. It is this flexible return process that allows us to examine how an investor, with a static type of narrow framing/loss aversion preferences, might react to an intertemporal budget constraint that goes far beyond Heston's (1993) stochastic volatility model as well as the increasingly more popular stochastic volatility with jump model (see, for example, Anderson, Benzoni, and Lund, 2002). The genesis of the proposed return process, which is designed specifically for stocks, can be described succinctly as follows: the unexpected changed in the future (stock) dividend growth is assumed to be the primary source of uncertainty underlying the (stock) return process and its conditional variance, referred to as the *fundamental volatility*, may persist (the well-known ARCH effect). An investor who anticipates higher future volatility will demand a larger return for holding this risky asset that in turn causes the current return to fall. Such a dynamic chain reaction has been referred to as *the volatility feedback effect* and the proposed model is therefore called the stochastic volatility feedback model. Since the fundamental volatility plays such an important role in the proposed model, it is regarded as the state variable which, together with the return itself, form a bivariate diffusion model. It should be stressed that, due to the volatility feedback effect, the covariance between the return and the state variable in the proposed bivariate model becomes a nonlinear function of the state variable and implies time-varying investment opportunities. Such changing investment opportunities will induce a rational investor, with or without narrow framing/loss aversion, to hedge against the resulting risks and therefore serve as a flexible analytic basis for the dynamic asset allocation decision.

Before the proposed return model can be used to derive any useful quantitative result about the intertemporal effects of narrow framing/loss aversion on asset allocation, we must first replace all the parameters of the model with empirically realistic values which may be obtained only through an empirical study. In this paper we employ Gallant and Tauchen's (1996, 2002) efficient method of moment estimation to estimate the proposed continuous-time model using S&P500 daily data from October 1982 to November 2004. In our empirical endeavor we also estimate stochastic volatility model and the stochastic volatility with jump model for the comparison purpose. Our empirical results unequivocally confirm the superiority of the proposed model, due to its flexibility in the time-varying conditional variances of returns and conditional covariances between returns and the state variable.

Once we equip the intertemporal budget constraint with empirically validated volatility feedback effects, we then conduct a detailed sensitivity analysis of the strategic asset allocation with respect to changes in the time horizon and in various parameters, of which the most important are the degree of narrow framing/loss aversion in preferences and the size of volatility feedback in the intertemporal budget constraint. The conclusion can be summarized as follows: in the absence of narrow framing/loss aversion, the myopic demand for the risky asset declines as the fundamental volatility (the state variable) increases, indicating the investor's typical response to increasing uncertainty. However, when narrow framing/loss aversion kicks in, the investor will become highly sensitive to volatility changes because large volatility under the volatility feedback effect might mean an opportunity of earning excess return. When the fundamental volatility gets sufficiently large so that the chance of earning excess return becomes large enough to overcome her fear due to loss aversion, the investor will raise her myopic demand for the risky asset. In other words, the volatility feedback effect can induce quite different responses towards volatility from an investor with narrow framing/loss aversion even in the short term.

As to the intertemporal effects of narrow framing/loss aversion, it is not surprising to find that they are mostly proportional to the size of the fundamental volatility and this relationship is particularly strong when the time horizon for allocation planning is long; that is, as the increasing fundamental volatility provides a greater opportunity for future returns, the intertemporal demand for the risky asset will rise much more rapidly than in the cases without the volatility feedback effect and without narrow framing/loss aversion and it is particularly so when the time horizon is long enough for the investor to take full advantage of the volatility feedback effect. One implication from this analysis is that whether loss aversion can explain the equity premium puzzle as argued by numerous authors not only depends on whether narrow framing is present or not, as suggested by Barberis and Huang (2003, 2004), but also depends on whether the investor is vigilant enough to respond to changing investment opportunities reflected by the volatility feedback effects.

Another useful finding from our analysis is that, because risk aversion, characterized typically by the constant relative risk aversion coefficient, is separated from loss aversion in our model, we can identify their respective effects on asset allocation and find that the effects of narrow framing/loss aversion are more dynamic than those of risk aversion. Specifically, we find that, irrespective of changes in the state variable, increasing risk aversion consistently results in reductions in investment, while increasing narrow framing/loss aversion causes investment, consumption, and savings all to become much more responsive to the changes in the state variable (especially under the volatility feedback effect). Consequently, we can expect a much larger trading volume over time under strong narrow framing/loss aversion than under large risk aversion.

In the next section we will first derive the solution to the dynamic asset allocation problem under narrow framing/loss aversion. There the optimal investment ratio is divided into the myopic and intertemporal components and separately analyzed. In section 3 we then propose the so-called the stochastic volatility feedback return model underlying the intertemporal budget constraint and estimate it using the efficient method of moment estimation. Equipped with empirically validated volatility feedback effects, section 4 proceeds with the sensitivity analysis of the optimal consumption, savings, welfare, as well as myopic demand and intertemporal hedge demand for the stock, with respect to changes in the time horizon, in various preference parameters, and in the volatility feedback effect. Section 5 contains a short summary.

2 Asset Allocation under Narrow Framing/Loss Aversion

Suppose an investor allocates her wealth W_t at time t over two assets – a riskfree asset with a constant rate of return $\bar{r}$ and a risky asset such that the dynamics of its price p_t is defined by the following general diffusion process:

$$\frac{dp_t}{p_t} = \mu_t^p\,dt + \sigma_{1t}^p\,dB_{1t} + \sigma_{2t}^p\,dB_{2t}, \tag{1}$$

where B_{1t} and B_{2t} are two Brownian motions,[2] while the drift μ_t^p and the diffusion σ_{1t} and σ_{2t} can be time-varying functions of some state variable h_t whose dynamics is defined by another diffusion process:

$$dh_t = \mu_t^h\,dt + \sigma_{1t}^h\,dB_{1t} + \sigma_{2t}^h\,dB_{2t}. \tag{2}$$

The possibility of including a state variable in the framework greatly enlarges the scope of our analysis. Given that the investor allocates the proportion ϕ_t of her wealth W_t to the risky asset, we assume that she has a time-additive expected utility function that is defined by the following indirect utility function over an infinitesimal time interval $[t,\ t+dt]$:

$$\begin{aligned} V_t &\equiv V(W_t, h_t, t) \\ &= \sup_{C_t,\phi_t}\left\{\frac{C_t^{1-\gamma}}{1-\gamma}\,dt + \nu\cdot\mathrm{E}_t\left\{K\left[\phi_t W_t\cdot\left(\frac{p_{t+dt}-p_t}{p_t} - \bar{r}\,dt\right)\right]\right\} + e^{-\tau\,dt}\mathrm{E}_t(V_{t+dt})\right\}, \end{aligned} \tag{3}$$

where C_t is the investor's consumption at time t, γ is the relative risk aversion (RRA) coefficient such that $\gamma > 0$ and $\gamma \neq 1$, and τ is the subjective discounting factor. The second term on the right-hand side shows the investor' narrow framing for which we make the following assumption:

Assumption 1 (Narrow Framing/Loss Aversion) *The coefficient ν indicates the degree of investor's concern about the risk of the risky asset in isolation while, given a number $\kappa > 1$, the loss aversion function is defined as follows:*

$$K(z) \equiv \begin{cases} z, & \text{if } z \geq 0, \\ \kappa\cdot z, & \text{otherwise.} \end{cases} \tag{4}$$

The piecewise-linear specification[3] of the K function reflects the investor's asymmetric valuation of the gain and the loss from the risky asset. The utility reduction the investor suffers

[2] Equipping the price process with more than one Brownian motion allows for more flexibility. Detailed specifications will be given in Section 2.

[3] Our specification is simpler than the loss aversion utility function proposed by Kahneman and Tversky (1979) in their prospect theory. Their K function can be concave for $z \geq 0$ and concave-convex for $z < 0$ while ours is linear (but with different slopes) in both domains .

from one dollar loss is larger than the utility increment she gets from one dollar gain; that is, losses loom larger than gains. Similar specification for narrow framing/loss aversion as an additional term in the utility function (3) has been considered in Barberis and Huang (2003, 2004). The argument of the K function in (3) is the instantaneous excess rate of return of the risky asset over the riskfree rate. In order words, the fixed riskfree rate $\bar{r}$ is assumed to be the so-called reference point for loss aversion.

The Hamilton-Jacobi-Bellman equation for (3) is presented in the following theorem whose proof is given in Appendix 1.

Theorem 1 *Suppose the value function $V(W_t, h_t, t)$ defined in (3) is twice continuously differentiable with respect to all its arguments and $\phi_t \geq 0$, then the corresponding Hamilton-Jacobi-Bellman equation for (3) as $dt \to 0$ is*

$$0 = \sup_{C_t, \phi_t} \left\{ \frac{C_t^{1-\gamma}}{1-\gamma} + \nu \cdot \phi_t W_t (\mu_t^p - \bar{r}) \left[P_t\left(\frac{dp_t}{p_t} \geq \bar{r}\, dt \right) - \kappa \cdot P_t\left(\frac{dp_t}{p_t} < \bar{r}\, dt \right) \right] - \tau \cdot V_t + \nabla V_t \right\},$$

with the terminal condition $V(W_T, h_T, T) = W_T^{1-\gamma}/(1-\gamma)$ at the terminal date T. Here ∇ denotes the differential generator and P_t denotes the conditional probability given the information up to time t.

Given the intertemporal budget constraint

$$dW_t = \left\{ W_t\left[\bar{r} + \phi_t(\mu_t^p - \bar{r})\right] - C_t \right\} dt + \phi_t W_t \left(\sigma_{1t}^p\, dB_{1t} + \sigma_{2t}^p\, dB_{2t} \right), \tag{5}$$

and the dynamics (2) of the state variable h_t, then

$$\nabla V_t = \dot{V} + V_w \left\{ W_t\left[\bar{r} + \phi_t(\mu_t^p - \bar{r})\right] - C_t \right\} + \frac{V_{ww} W_t^2}{2} \sigma_{pt}^2 \phi_t^2 + V_{wh} W_t \sigma_{pht} \phi_t + V_h \mu_t^h + \frac{V_{hh}}{2} \sigma_{ht}^2, \tag{6}$$

where $\dot{V} \equiv \partial V(W_t, h_t, t)/\partial t$, $V_w \equiv \partial V(W_t, h_t, t)/\partial W_t$, $V_h \equiv \partial V(W_t, h_t, t)/\partial h_t$, and V_{ww}, V_{wh}, and V_{hh} are the corresponding second order partial derivatives. Moreover, σ_{pt}^2 and σ_{ht}^2 are instantaneous variance of dp_t/p_t and dh_t, respectively, whereas σ_{pht} is their instantaneous covariance.

Given the standard assumption that the value function has the following separable functional form

$$V(W_t, h_t, t) = A(h_t, t) \cdot \frac{W_t^{1-\gamma}}{1-\gamma}, \tag{7}$$

for some function $A(\cdot, \cdot)$, it is straightforward to derive the optimal consumption-wealth ratio

$$\left(\frac{C_t}{W_t} \right)^* = A(h_t, t)^{-1/\gamma}, \tag{8}$$

and the optimal portfolio weight

$$\phi_t^* = \phi_{Mt}^* + \phi_{Ht}^*, \tag{9}$$

where

$$\phi_{Mt}^* \equiv \left(\frac{\mu_t^p - \bar{r}}{\sigma_{pt}^2}\right)\cdot\left(\frac{1}{\gamma}\right)\left\{1 + \frac{\nu}{V_w}\left[P_t\left(\frac{dp_t}{p_t} \geq \bar{r}\,dt\right) - \kappa\cdot P_t\left(\frac{dp_t}{p_t} < \bar{r}\,dt\right)\right]\right\} \tag{10}$$

and

$$\phi_{Ht}^* \equiv \frac{\sigma_{pht}}{\sigma_{pt}^2}\cdot\frac{A_h}{\gamma\cdot A}. \tag{11}$$

In the above expressions $V_w = A/W_t^\gamma$ is the marginal utility of wealth whereas A is a function satisfying the following nonlinear partial differential equation:

$$A\left[\gamma A^{-1/\gamma} + (1-\gamma)\left(\bar{r} + \frac{\gamma}{2}\sigma_{pt}^2\,\phi_t^{*2}\right) - \tau\right] + \dot{A} + A_h\mu_t^h + \frac{1}{2}A_{hh}\,\sigma_{ht}^2 = 0, \tag{12}$$

where $\dot{A} \equiv \partial A/\partial t$, $A_h \equiv \partial A/\partial h_t$, and $A_{hh} \equiv \partial^2 A/\partial h_t^2$.

The closed-form expression for ϕ_t^* requires knowledge of the A function and its partial derivative A_h, which can be solved from the nonlinear partial differential equation (12). We notice that among the two additive terms of the optimal portfolio weight ϕ_t^* in (9) the ϕ_{Mt}^* term is almost independent of the A function. It is worthwhile to further examine this term which itself is the product of three components. The first component is usually referred to as the risk price of the risky asset (adjusted by the riskfree rate) $(\mu_t^p - \bar{r})/\sigma_{pt}^2$, which is generally viewed as the on-going market compensation for risk. The second component is reciprocal to the RRA coefficient γ which obviously reflects the inverse relationship between the degree of risk aversion and the desired amount of the risky asset.

The most interesting part is the third component which consists of the uneven difference in the two complementary conditional probabilities of instantaneous changes in return resulted from narrow framing/loss aversion and is inversely related to the marginal utility of wealth $V_w = A/W_t^\gamma$. The interpretation of the reciprocal of V_w is straightforward: if the investor's marginal utility of wealth is large, then she would be more concerned with the risk contained in the risky asset. However, the appearance of such V_w renders the partial differential equation (12) almost impossible to solve even numerically. In order to simplify the analysis as well as to improve the precision of the numerical solution to the partial differential equation (12), we adopt the following assumption:

Assumption 2 *The coefficient ν is proportional to marginal utility of wealth $\nu = \nu_\circ V_w = \nu_\circ A/W_t^\gamma$, with a positive constant $\nu_\circ$.*

In other words, the larger is the investor's marginal utility of wealth, the more is she concerned with the risk in isolation. Similar assumptions leading to a homothetic valuation function and a tractable solution to the partial differential equation have also been made by Maehout (2001). Under Assumption 2 the term ν/V_w reduces to a constant $\nu_\circ$ so that it becomes possible not only to solve the partial differential equation (12) for A (as will be seen later in Section 4) but also to provide a clearer interpretation for the term ϕ^*_{Mt} in (10). For example, the term ϕ^*_{Mt} is now completely independent of the A function so that it will not be affected, at least directly, by any possible future changes in the investment opportunities over the long run. We can therefore refer to ϕ^*_{Mt} as the myopic demand for the risky asset to stress its short-run nature.

We are especially interested in the third component of the myopic demand ϕ^*_{Mt} resulted from narrow framing/loss aversion so that we denote it as

$$n_t \equiv 1 + \nu_\circ \left[P_t\left(\frac{dp_t}{p_t} \geq \bar{r}\,dt\right) - \kappa \cdot P_t\left(\frac{dp_t}{p_t} < \bar{r}\,dt\right)\right]. \tag{13}$$

Here we note that dp_t/p_t is approximately equal to $\mu^p_t + \sigma_{pt}\cdot z_t$, where z_t is a standard Gaussian random variable, so that the probability of having an instantaneous rate of return that is greater than or equal to the riskfree rate, denoted as π_t, can be expressed as

$$P_t\left(\frac{dp_t}{p_t} \geq \bar{r}\,dt\right) = 1 - P_t\left(\frac{dp_t}{p_t} < \bar{r}\,dt\right) = \Phi\left(\frac{\mu^p_t - \bar{r}}{\sigma_{pt}}\right) \equiv \pi_t, \tag{14}$$

where $\Phi(\cdot)$ is the cumulative distribution function of the standard Gaussian distribution and $(\mu^p_t - \bar{r})/\sigma_{pt}$ is the well-known Sharpe ratio for the risky asset. Given π_t we can then rewrite n_t as follows:

$$\begin{aligned} n_t &= 1 + [\pi_t - \kappa(1-\pi_t)]\cdot\nu_\circ \\ &= (1 + \nu_\circ\,\pi_t) - \nu_\circ(1-\pi_t)\cdot\kappa \\ &= (1 - \nu_\circ\,\kappa) + \nu_\circ(1+\kappa)\cdot\pi_t. \end{aligned} \tag{15}$$

From the first equality we learn that whether n_t is an increasing or decreasing function of the narrow framing intensity $\nu_\circ$ depends on whether the loss aversion parameter κ is smaller or greater than the odds ratio $\pi_t/(1-\pi_t)$ of earning an instantaneous return that is higher than the riskfree rate. The intuition is as follows: when the odds of earning excess return is larger than the degree of adverse feeling pertinent to the loss, then a narrow framing investor will acquire so much risky asset that its risk cannot be accounted for by the market compensation for risks. But when the odds of earning excess return becomes relatively lower, she will also overreact by excessively cutting back the investment in the risky asset.[4] The second equality implies that n_t is inversely related to the loss aversion parameter κ, which obviously reflects the inhibitive effects of loss aversion on the demand for the risky asset. The third equality indicates

[4]Through experiments Tversky and Kahneman (1992) suggest that the loss aversion parameter under the prospect theory should be 2.25. If so, then under-investment will occur so long as the probability of earning excess return π_t is less than about 0.692. The loss aversion parameter considered by Berkelaar, Kouwenberg, and Post (2004) and by Benartzi and Thaler (1995) are, respectively, 2.5 and 2.77. The corresponding threshold values of π_t will then be 0.714 and 0.735.

that n_t is a positive-sloped linear function of π_t so that the myopic demand for the risky asset is positively related to the probability of earning excess return. An important inference we draw from this analysis of (15) is that, although the two concepts of narrow framing and loss aversion are usually abbreviated as a single phrase as in this paper, their respective parameters $\nu_\circ$ and κ actually play distinctively different roles on asset allocation. Loss aversion definitely has a depressing effect on the demand for the risky asset. But how narrow framing affects the investor's allocation decision turns out to be much more complicated. To further investigate how versatile the combined effects of narrow framing/loss aversion on asset allocation might be, we need numerical examples which will be provided later in Section 4.

We conclude that the myopic demand for the risky asset ϕ^*_{Mt} is a product of three components. The first component is proportional to the current risk price of the risky asset $(\mu^p_t - \bar{r})/\sigma^2_{pt}$ that represents market compensation for risk within the current investment opportunity set. Current market information can influence the myopic demand mainly thorough this component. In contrast, the preference parameters γ, $\nu_\circ$, and κ cling to the other two components which jointly can be viewed as the amount of risk an investor is willing to take.[5] In other words, the myopic demand for the risky asset is nothing but the product of the risk price under current market conditions and the amount of risk the investor is willing to take.

Similar to the decomposition of the myopic demand ϕ^*_{Mt}, the ϕ^*_{Ht} term in (11) is also a product of two parts in which market information exerts its influence mainly through the first part $\sigma_{pht}/\sigma^2_{pt}$ while the preference parameters γ, $\nu_\circ$, and κ work only through the second part $A_h/\gamma A$. However, it is much more interesting to explore the difference between ϕ^*_{Ht} and ϕ^*_{Mt} for which we have three observations.

We first note that, apart from the variance σ^2_{pt}, market information affects the myopic demand ϕ^*_{Mt} completely through the drift term $(\mu^p_t - \bar{r})$ of the price process while it is mainly the covariance σ_{pht} between the price process and the state variable h_t that carries the effects of market information to the ϕ^*_{Ht} term. Hence, the determination of the myopic demand ϕ^*_{Mt} is more straightforward and is based on information of the price process alone, while the decipherment of the ϕ^*_{Ht} term is more demanding and requires the knowledge about how the price process is correlated with the state variable h_t. Second, being independent of the subjective discounting factor τ and the terminal date T that characterize the dynamics of the asset allocation, the myopic demand ϕ^*_{Mt} is obviously a static concept as mentioned earlier. In contrast, the ϕ^*_{Ht} term is necessarily of the dynamic nature since it contains the percentage marginal utility of the state variable $A_h/A = \partial \ln A/\partial h_t = \partial \ln V/\partial h_t$ that must be solved from the partial different equation (12) in which both T and τ play crucial roles. That is, the ϕ^*_{Ht} term can be fully explained only after the time dimension is incorporated into the analysis. Third, the way the three main preference parameters γ, $\nu_\circ$, and κ affect the myopic demand ϕ^*_{Mt} is quite explicit and clear-cut as indicated in (10) and (13). But the effects of preference parameters on the ϕ^*_{Ht} term are all hidden in the percentage marginal utility of the state variable A_h/A and cannot be

[5]Market information can also affect the third component n_t through the Sharpe ratio and then the probability π_t. However, what affects the n_t component most is still the values of the narrow framing/loss aversion parameters.

separately analyzed.

Since the first part of the ϕ^*_{Ht} term involves the correlation between the asset price and the state variable h_t, it seems quite natural to include the investor's sensitivity toward h_t, i.e., A_h/A, as the second part. Intuitively, because the state variable h_t is correlated with the stock price, it is possible for the investor to assess the time-varying opportunity of earning future returns by observing h_t. The investor's sensitivity with respect to h_t in turn reveals how she would react to such an investment opportunity. Consequently, the ϕ^*_{Ht} term, as a product of these two parts, is referred to as the investor's intertemporal hedge demand for stock.

Although the n_t term does not explicitly show up in (11) for ϕ^*_{Ht}, we cannot overlook the effects of narrow framing/loss aversion on the intertemporal hedge demand. It is also necessary to evaluate more precisely how different specifications of the preference parameters might affect the intertemporal hedge demand. But to do so requires numerical evaluation of the percentage marginal utility of the state variable A_h/A which in turn calls for full specification of the return process (1) and the state variable process (2) in the intertemproal budget constraint (5). This will be proceeded in the next section. It goes without saying that any assumptions we make about the intertemproal budget constraint will be as important to the dynamic asset allocation as the narrow framing/loss aversion assumption we have made about the investor's preferences.

3 The Specification of the Intertemporal Budget Constraint

In this section we will first propose and then estimate new continuous-time specifications for the return process (1) and the state variable process (2) in the intertemproal budget constraint (5). The estimated model will then be used for a thorough quantitative analysis of asset allocation in the next section continued from the previous section. Here before presenting the proposed model, we shall briefly review two popular diffusion systems in the literature and comment on the reasons why they are not adopted in our later analysis.

A very common and simple specification of the diffusion processes is the stochastic volatility (SV) model first suggested by Heston (1993):

$$\begin{bmatrix} dy_t \\ dh_t \end{bmatrix} = \begin{bmatrix} \delta_\circ + \delta_1 h_t \\ \psi_\circ - \psi_1 h_t \end{bmatrix} dt + \begin{bmatrix} \sqrt{h_t} & 0 \\ \rho\sigma\sqrt{h_t} & \sigma\sqrt{1-\rho^2}\sqrt{h_t} \end{bmatrix} \begin{bmatrix} dB_{1t} \\ dB_{2t} \end{bmatrix}, \tag{16}$$

where y_t denoted the log price of the risky asset[6] (i.e., $y_t \equiv \ln p_t$) whereas the state variable h_t is the return volatility. In other words, it is the instantaneous return variance σ^2_{pt} of y_t that is assumed to be the state variable. In the drift part of this bivariate system, the δ_1 parameter characterizes the trade-off between the return and the risk while the ψ_1 parameter indicates how fast volatility reverts to its mean. From the diffusion part we also note that the instantaneous

[6]We define the return process in terms of the log price differential $dy_t = d\ln p_t$, instead of dp_t/p_t, to facilitate its estimation later in Subsection 3.3.

variance σ_{ht}^2 of the change in volatility is $\sigma^2 h_t$ while the instantaneous correlation between return and the change in volatility is ρ which is time-invariant.

Plugging these σ_{pt}^2, σ_{ht}^2, as well as σ_{pht} back to (9) and (12) yields relatively simple expressions which can be used to solve for the optimal portfolio weight ϕ_t^* numerically. We shall make two quick comments on the drawbacks of the SV model while leaving more details to Section 4. First, as pointed by Liu (2001) the intertemporal hedge demand for the risky asset in the optimal portfolio weight ϕ_t^* of (9) from the SV model is almost always unreasonably small in comparison with the myopic demand irrespective the status of the state variable. Secondly, Anderson, Benzoni, and Lund (2002) and Chernov, Gallant, Ghysels, and Tauchen (2003) all point out that the SV model does not fit data well. Because of these two unsatisfactory features of the SV model, many researchers, e.g., Duffie, Singleton, and Pan (2001), Eraker (2004), and Liu, Longstaff, and Pan (2003), have considered affine jump-diffusion models. In particular, Anderson, Benzoni, and Lund (2002) introduce a jump component into the SV model (16) to enhance its empirical performance:

$$\begin{bmatrix} dy_t \\ dh_t \end{bmatrix} = \begin{bmatrix} (\delta_\circ - \zeta) + \delta_1 h_t \\ \psi_\circ - \psi_1 h_t \end{bmatrix} dt + \begin{bmatrix} \sqrt{h_t} & 0 \\ \rho\sigma\sqrt{h_t} & \sigma\sqrt{1-\rho^2}\sqrt{h_t} \end{bmatrix} \begin{bmatrix} dB_{1t} \\ dB_{2t} \end{bmatrix} + \begin{bmatrix} J_t \\ 0 \end{bmatrix} dq_t, \tag{17}$$

which is usually referred to as the stochastic volatility with jump (SVJ) model. The added jump term contains a discrete jump process q_t that is independent of the two included Brownian motions B_{1t} and B_{2t} and is defined by $P_t(dq_t = 1) = \zeta\, dt$, where the parameter ζ represents the jump intensity. The scaling factor J_t characterizes the jump size at time t and is assumed to be independent of q_t and have a log-normally distribution such that $\ln(1+J_t) \sim \mathcal{N}(-0.5\,\varphi^2,\ \varphi^2)$, where φ is an additional parameter.

While the instantaneous return variance $\sigma_{pt}^2 = h_t + \zeta\cdot[\exp(\varphi^2) - 1]$ is more versatile than its counterpart in the SV model so that the empirical performance of the SVJ model does have the potential to greatly improve (as will be shown later in Subsection 3.3), we should not overlook the fact that behavioral and theoretical justification for adding a jump component is not readily available. In other words, the jump component is largely an empirically motivated device. It is then not surprising to find it difficult to conduct asset allocation analysis based on a SVJ return process (even without considering narrow framing restraint). See for example Liu, Longstaff, and Pan (2003) and Das and Uppal (2004).

Given the drawbacks of the SV and the SVJ models, we cannot help but to look for a new specification with sufficiently flexible structure that allows us to analyze the effect of narrow framing/loss aversion. With this objective in mind, we choose to construct a diffusion model based on a discrete-time model for stock returns proposed by Campbell and Hentschel (1992).

3.1 The Discrete-Time Specification

Let us denote the log stock return and the log dividend at time t by r_t and d_t, respectively. So long as the variation in the log dividend-price ratio is not too great, the unexpected stock return can be approximated by the following equality:[7]

$$r_{t+1} - \mathrm{E}_t(r_{t+1}) = (\mathrm{E}_{t+1} - \mathrm{E}_t)\sum_{j=0}^{\infty}\xi^j \Delta d_{t+1+j} - (\mathrm{E}_{t+1} - \mathrm{E}_t)\sum_{j=1}^{\infty}\xi^j r_{t+1+j}, \qquad (18)$$

where the discounting factor ξ is the average ratio of the stock price to the sum of the stock price and the dividend. What approximation (18) says is that an unexpected change in the stock return on the left-hand side can be attributed to the unexpected change in the future dividend growth and the unexpected change in future returns (with a negative sign). More specifically, a positive unexpected dividend announcement will raise today's stock price and then increase the unexpected return. In contrast, a positive unexpected future return will increase today's expected stock return and reduce unexpected return.

Campbell and Hentschel (1992) proposed their model by making an assumption for each of the two terms on the right-hand side of (18). The first term on the right-hand side of (18), i.e., the unexpected change in the future dividend growth, is assumed to have no serial correlations at the level but a lot of them in the volatility:

$$(\mathrm{E}_{t+1} - \mathrm{E}_t)\sum_{j=0}^{\infty}\xi^j \Delta d_{t+1+j} = \sqrt{h_{t+1}} \cdot v_{t+1}, \qquad (19)$$

where v_{t+1} are assumed to be i.i.d. Gaussian innovations with zero mean and unit variance. The h_{t+1} term is the conditional variance of the unexpected change in the future dividend growth and is generated by the following quadratic GARCH process:

$$h_{t+1} = \omega + \alpha(\sqrt{h_t} \cdot v_t - \eta)^2 + \beta h_t, \qquad (20)$$

where α is the ARCH parameter and β the GARCH parameter.[8] The η parameter plays a particularly important role in this nonstandard GARCH model. If it has a positive value, as we usually assume it is, then the effect of a negative shock v_t on h_{t+1} is necessarily larger than that of a positive one. In other words, the size of the η parameter represents the degree of volatility asymmetry in response to the past shock and we refer to η as the *leverage effect*.

The second assumption Campbell and Hentschel (1992) made has to do with the trade-off between risk and return in that the expected stock return is assumed to be a linear function of volatility of the future dividend growth :

$$\mathrm{E}_t(r_{t+1}) = \delta_\circ + \delta_1 h_{t+1}, \qquad (21)$$

where the slope δ_1 is assumed to have a positive value to reflect the fact that larger anticipated future volatility calls for higher required return for holding stock.

---

[7]The derivation can be found in Campbell and Shiller (1988) and Campbell (1991). Here we have assumed $\lim_{j\to\infty}\xi^j r_{t+j} = 0$ as a terminal condition.

[8]Their sum $\alpha + \beta$ must be smaller than one but is usually quite close to one, reflecting the high degree of persistence in h_{t+1}.

By repeated substitution using (21), it is possible to derive the following expression for the unexpected change in future returns, i.e., the second term on the right-hand side of (18):

$$(\mathrm{E}_{t+1} - \mathrm{E}_t)\sum_{j=1}^{\infty} \xi^j r_{t+1+j} = -2\eta\lambda\sqrt{h_{t+1}}\cdot v_{t+1} + \lambda h_{t+1}(v_{t+1}^2 - 1), \tag{22}$$

where

$$\lambda = \frac{\alpha\xi\delta_1}{1-\xi(\alpha+\beta)} > 0. \tag{23}$$

As a result, we have the following return process:

$$r_{t+1} = \delta_\circ + \delta_1 h_{t+1} + (1+2\eta\lambda)\sqrt{h_{t+1}}\cdot v_{t+1} - \lambda h_{t+1}(v_{t+1}^2 - 1). \tag{24}$$

It is important to note that the innovation v_{t+1} in the future dividend growth is the only source of uncertainty and the corresponding conditional variance h_{t+1} can then be referred to as "fundamental volatility."

The last term in (24) implies that any unexpected change in the future dividend growth v_{t+1}, be it positive or negative, will result in a reduction in the current return. The intuition is as follows: an unexpected change in the future dividend growth means rising volatility. Since volatility persists (due to the GARCH effect given in (20)), an investor who anticipates higher future volatility will demand larger return for holding stock (based on the tradeoff between risk and return (21)), which in turn causes current return to fall (due to the second term on the right-hand side of (18)). Such a dynamic chain reaction has been referred to as the *volatility feedback effect* (Campbell and Hentschel described it as "no news is good news"). As opposed to such a depressing effect, we note that the third term on the right-hand side of (24) causes the return to move in the same direction as v_{t+1}. As a result, the influence of a negative v_{t+1} on the return is necessarily larger than that of a positive one.[9] Since the η parameter appears in the third term, we conclude that the leverage effect (asymmetric effects of the past shock on the volatility h_{t+1}) contributes to the asymmetry in stock return's response to the past shock. In contrast, the volatility feedback effect λ, appearing in both the last two terms of (24), determines the magnitude of return's total asymmetric response to the past shock.

It is interesting to note that the definition (23) of the λ parameter consists of the three structural parameters α, ξ, and δ_1 as its numerator, and is also directly related to the size of $\alpha+\beta$ in the denominator. The composition of the λ parameter clearly shows that the volatility feedback effect is a result of combining persistent volatility (characterized by the ARCH effect α as well as the GARCH effect β), dynamics (represented by the discounting factor ξ), as well as the trade-off between risk and return (implied by the δ_1 parameter). Noticeably absent from this construction is the leverage effect η. Obviously, the volatility feedback effect is a concept independent of the leverage effect.

---

[9] Campbell and Hentschel (1992) indicated that the conditional skewness of returns in (24) is indeed negative and is equal to $-[6(1+2\eta\lambda)^2\lambda h_t^2 + 8\lambda^3 h_t^3]/[(1+2\eta\lambda)^2 h_t + 2\lambda^2 h_t^2]^{3/2}$ while the excess kurtosis is also positive and is equal to $[48(1+2\eta\lambda)^2\lambda^2 h_t^3 + 48\lambda^3 h_t^3]/[(1+2\eta\lambda)^2 h_t + 2\lambda^2 h_t^2]^2$.

3.2 The Continuous-Time Model

In this subsection we will present the continuous-time counterparts of the stock return process given in (24) and a state variable process defined by (20). By adopting Nelson (1990, 1992), Nelson and Foster (1994), and Duan's (1997) methodology, we are able to show that, under some mild regularity conditions, (24) and (20) converge to the following bivariate diffusion system (the derivation is given in the Appendix 2):

$$\begin{bmatrix} dy_t \\ dh_t \end{bmatrix} = \begin{bmatrix} \delta_\circ + \delta_1 h_t \\ \psi_\circ - \psi_1 h_t \end{bmatrix} dt + \begin{bmatrix} (1+2\eta\lambda)\sqrt{h_t} & -\sqrt{2}\,\lambda h_t \\ -2\alpha\eta\sqrt{h_t} & \sqrt{2}\,\alpha h_t \end{bmatrix} \begin{bmatrix} dB_{1t} \\ dB_{2t} \end{bmatrix}, \qquad (25)$$

where we assume $dy_t/dt = r_t$. The system contains two reduced-form parameters: $\psi_\circ \equiv \omega + \alpha\eta^2$ and $\psi_1 \equiv 1 - \alpha - \beta$. While the discrete-time models (24) and (20) only have one source of uncertainty – the innovation v_t from the unexpected change in the future dividend growth, their continuous-time counterpart (25) contains two independent Brownian motions B_{1t} and B_{2t} representing two random sources.[10]

It is easy to show that the instantaneous variances of the stock return and the change in volatility are, respectively,

$$\sigma_{pt}^2 = \big[(1+2\eta\lambda)^2 + 2\lambda^2 h_t\big] h_t, \qquad (26)$$

and

$$\sigma_{ht}^2 = 2\alpha^2(2\eta^2 + h_t) h_t, \qquad (27)$$

while the instantaneous covariance between stock return and the change in volatility is negative:

$$\sigma_{pht} = -2\alpha\big[(1+2\eta\lambda)\eta + \lambda h_t\big] h_t < 0. \qquad (28)$$

All of these moments are quadratic functions of the state variable h_t. It is also clearly seen that the influence of the volatility feedback effect λ is much larger than that of the leverage effect η as argued earlier. We therefore refer to the proposed model (25) as the *stochastic volatility feedback* (SVF) model.

Thanks to the volatility feedback effect λ (and to a lesser extent the leverage effect η), the instantaneous variance of the stock return in (26) is larger, sometimes substantially larger, than the fundamental volatility h_t corresponding to the future dividend growth and implies excessive volatility in the stock return observed by Shiller (1981).[11] Also note that Bekaert and Wu (2000) and Wu (2001) have found some empirical evidence supporting negative relationship

[10] Since there is only one risky asset in our framework, the market seems to be complete in the discrete-time but becomes incomplete when it converges to the continuous-time limit. Also, the instantaneous skewness and the excess kurtosis of the return will be the same as the standard normal distribution.

[11] It should be clear by now that the state variable h_t in the SV and SVJ model is the stock return volatility. In contrast, the state variable h_t in the SVF model is the conditional variance of unexpected change in the future dividend growth as defined in (19).

between stock return and the change in volatility. Besides their empirical relevance we should stress that the sophisticated structure in these moments can be quite useful for our analysis of the dynamic asset allocation problem as will be shown in Section 4. Intuitively, the existence of a nonlinear relationship between the covariance σ_{pht} and the state variable h_t implies time-varying investment opportunities for a long term investor who certainly will attempt to hedge against the risk resulted from such changing investment opportunities.

By comparing the above instantaneous variance of the change in volatility σ_{ht}^2 as well as the covariance σ_{pht} of the SVF model with those of the SV model, we immediately realize that the fixed σ^2 and ρ parameters in the SV model are comparable to the terms $2\alpha^2(2\eta^2 + h_t)$ and $-\sqrt{2\eta^2/(2\eta^2 + h_t)}$ of the SVF model, respectively. We can then identify the σ^2 parameter and the correlation coefficient ρ of the SV model respectively with the ARCH effect and the leverage effect; i.e., the α and η parameters respectively in the SVF model. Once we recognize such similarity between the SV model and the SVF model, it becomes clear that the SVF model differs from the SV models mainly in the volatility feedback effect λ, which can be motivated by the three well-established concepts of volatility persistence, dynamics, as well as the trade-off between risk and return.[12] We also believe it is this theoretical interpretation that offers stronger justification for the volatility feedback effect and provides broader analytic scope than what the SV model as well as the empirically-motivated jump component in the SVJ model could ever have.

Before we can plug the above moments of the SVF model into the optimal portfolio weight ϕ_t^* in (9) and conduct further analysis, we must first replace parameters, the volatility feedback effect λ in particular, with empirically realistic values. In the next subsection we will estimate the parameters of the SVF model using daily stock price data. In this econometric undertaking we will also try to secure empirical evidence supporting the superiority of the SVF model over its two competitors – the SV model and the SVJ model.

3.3 The Estimation of the Diffusion Processes

We use S&P500 stock index daily return from October 20, 1982 to November 16, 2004 to estimate the proposed SVF model, as well as the SV and SVJ models as benchmarks. The sample size is 5,572. The return (the log-difference of the original price date) data are shown in the upper panel of Figure 1 (on page 21). The basic statistics of the sampled daily returns are as follows: the sample average is 0.038, the standard deviation, skewness, and kurtosis are 1.069, −1.921, and 42.1235, respectively. The traditional maximum likelihood estimation (MLE) is difficult to implement in estimating continuous-time diffusion models like the SVF, SV, and SVJ models with discrete-time sampled observations even if we can come up with discrete approximations to the models. This is because closed-form likelihood functions for such discrete approximations are generally not available. A variety of estimation approaches have

[12] However, the SV model is not a special case of the SVF model because the diffusion parameters associated with dB_{2t} contain $\sqrt{h_t}$, instead of h_t, in the SV model.

been suggested in the literature to solve this problem, among which are non-parametric methods proposed by Ait-Sahalia (1996) and Hansen and Scheikman (1995); the Markov chain Monte Carlo (MCMC) method used by Eraker (2001) and Elerian, Chib, and Shephard (2001); and simulation-based methods suggested by Duffie and Singleton (1993) and Gallant and Tauchen (1996, 2002).

In this paper we adopt Gallant and Tauchen's (1996, 2002) efficient method of moments (EMM) estimation to estimate the parameters, denoted by the vector $\boldsymbol{\theta}$, of the proposed SVF model (or alternatively the SV model or the SVJ model). The EMM procedure entails two steps – the projection step and the estimation step. In the projection step we first propose an auxiliary model for the data y_t, $t = 1, \ldots, T$, in terms of a conditional density function $f(y_t \mid Y_{t-1}, \boldsymbol{\gamma})$, where Y_{t-1} denotes the information set up to time $t-1$ and $\boldsymbol{\gamma}$ is the corresponding parameter vector, and then apply the quasi-maximum likelihood estimation to obtain an estimate $\hat{\boldsymbol{\gamma}}$ of $\boldsymbol{\gamma}$. Based on suggestions made by Anderson and Lund (1997), van der Sluis (1997), Anderson, Benzoni, and Lund (2002), we adopt the following specification for the auxiliary density function:

$$f(y_t \mid Y_{t-1}, \boldsymbol{\gamma}) = \frac{p(z_t)^2 + \epsilon}{\displaystyle\int_{-\infty}^{\infty} p(x)^2\, \phi(x)\, dx + \epsilon} \cdot \frac{\phi(z_t)}{s_t}, \tag{29}$$

where $\phi(x)$ is the density function of the standard normal distribution, $\epsilon = 0.0001$ is used to stabilize the numerical computation,[13] $z_t = (y_t - m_t)/s_t$, and

$$\begin{aligned} m_t &= a_\circ + a_1 y_{t-1}, \\ \ln s_t^2 &= b_\circ + \left[c_1 z_{t-1} + c_2 \left(|z_{t-1}| - \sqrt{\frac{2}{\pi}} \right) \right] \\ &\qquad + b_1 \left[c_1 z_{t-2} + c_2 \left(|z_{t-2}| - \sqrt{\frac{2}{\pi}} \right) \right] + b_2 \ln \sigma_{t-1}^2. \end{aligned}$$

That is, y_t is assumed to be follow an AR(1)-EGARCH(1,1) model.[14] Finally, we define $p(x)$ as follows:

$$p(x) \equiv \sum_{i=0}^{8} d_i \left(\sum_{j=0}^{[i/2]} \frac{(-1)^j \sqrt{i!}}{j!\, 2^{j\,(i-2j)!}} x^{i-2j} \right),$$

which is an orthogonal Hermite polynomial such that $\int_{-\infty}^{\infty} p(x)^2 \phi(x)\, dx = \sum_{i=0}^{8} d_i^2$. This polynomial can track down excess kurtosis and, to a lesser extent, skewness in the return data

[13]Gallant and Tauchen (2002) advise that the practice of adding ϵ can be quite important in numerical implementation of the EMM estimation, which was first suggested by Dai and Singleton (2000).

[14]We have experimented with various specifications in the class of AR(m)-EGARCH(p, q) and picked the AR(1)-EGARCH(1,1) model based on the BIC criterion.

that haven't been captured by the EGARCH part. As a summary we note that the parameter vector $\boldsymbol{\gamma}$ includes 15 parameters: two AR coefficients $a_\circ$, a_1; five EGARCH coefficients $b_\circ$, b_1, b_2, c_1, c_2; and eight Hermite coefficients $d_1, \ldots, d_8$ (d_0 has been normalized to 1). The same auxiliary specification will be used to estimate the three models: the SV, SVJ, and SVF models.

In the estimation step we first use the proposed model, (i.e., the SVF model or the SV model or the SVJ model), for a given value of the parameter vector $\boldsymbol{\theta}$, to simulate N artificial data $\hat{y}_i(\boldsymbol{\theta})$, $i = 1, \ldots, N$, and then consider minimizing the following quadratic form with respect to $\boldsymbol{\theta}$:

$$\min_{\boldsymbol{\theta}} \ \mathbf{m}(\boldsymbol{\theta} \mid \hat{\boldsymbol{\gamma}})' \, \boldsymbol{\Omega}(\hat{\boldsymbol{\gamma}})^{-1} \mathbf{m}(\boldsymbol{\theta} \mid \hat{\boldsymbol{\gamma}}), \tag{30}$$

where

$$\mathbf{m}(\boldsymbol{\theta} \mid \hat{\boldsymbol{\gamma}}) \equiv \frac{1}{N} \sum_{i=1}^{N} \frac{\partial \ln f(\hat{y}_i(\boldsymbol{\theta}) \mid Y_{t-1}, \hat{\boldsymbol{\gamma}})}{\partial \boldsymbol{\gamma}},$$

and

$$\boldsymbol{\Omega}(\hat{\boldsymbol{\gamma}}) \equiv \frac{1}{T} \sum_{t=1}^{T} \left[\frac{\partial \ln f(y_t \mid Y_{t-1}, \hat{\boldsymbol{\gamma}})}{\partial \boldsymbol{\gamma}} \right] \left[\frac{\partial \ln f(y_t \mid Y_{t-1}, \hat{\boldsymbol{\gamma}})}{\partial \boldsymbol{\gamma}} \right]'.$$

The solution, denoted by $\hat{\boldsymbol{\theta}}$, is the EMM estimate of $\boldsymbol{\theta}$. Under some regularity conditions, the EMM estimator is consistent and asymptotically normally distributed with a variance-covariance matrix which can be estimated by

$$\left[\mathbf{M}(\hat{\boldsymbol{\theta}} \mid \hat{\boldsymbol{\gamma}})' \, \boldsymbol{\Omega}(\hat{\boldsymbol{\gamma}})^{-1} \mathbf{M}(\hat{\boldsymbol{\theta}} \mid \hat{\boldsymbol{\gamma}}) \right]^{-1},$$

where $\mathbf{M}(\boldsymbol{\theta} \mid \hat{\boldsymbol{\gamma}}) \equiv \partial \mathbf{m}(\boldsymbol{\theta} \mid \hat{\boldsymbol{\gamma}}) / \partial \boldsymbol{\theta}$. When simulating the artificial data, we generate 55,000 data from the proposed continuous-time model with the time interval of $1/10$ per day and then drop the first 5,000. Hence, the number N in our estimation is 50,000.

The EMM approach can achieve the same level of asymptotic efficiency as the MLE given that $\mathbf{m}(\boldsymbol{\theta} \mid \boldsymbol{\gamma})$ is sufficiently close to the score function of the true model. Moreover, when the number a of the parameters in the auxiliary model (i.e., the number of the elements in the $\boldsymbol{\gamma}$ vector which is 15 in our specification) is greater than the number b of the parameters in the proposed model (i.e., the number of the elements in the $\boldsymbol{\theta}$ vector), then the statistic

$$C \equiv T \cdot \mathbf{m}(\hat{\boldsymbol{\theta}} \mid \hat{\boldsymbol{\gamma}})' \, \boldsymbol{\Omega}(\hat{\boldsymbol{\gamma}})^{-1} \mathbf{m}(\hat{\boldsymbol{\theta}} \mid \hat{\boldsymbol{\gamma}})$$

converges to a χ^2 distribution with $a - b$ degrees of freedom if the proposed model is true. This result can therefore be used to test the truthfulness of the proposed model. Finally, the statistic

$$t_i \equiv \frac{\sqrt{T} \cdot m_i(\hat{\boldsymbol{\theta}} \mid \hat{\boldsymbol{\gamma}})}{\sqrt{\left[\boldsymbol{\Omega}(\hat{\boldsymbol{\gamma}}) - \mathbf{M}(\hat{\boldsymbol{\theta}} \mid \hat{\boldsymbol{\gamma}}) \left[\mathbf{M}(\hat{\boldsymbol{\theta}} \mid \hat{\boldsymbol{\gamma}})' \boldsymbol{\Omega}(\hat{\boldsymbol{\gamma}})^{-1} \mathbf{M}(\hat{\boldsymbol{\theta}} \mid \hat{\boldsymbol{\gamma}}) \right]^{-1} \mathbf{M}(\hat{\boldsymbol{\theta}} \mid \hat{\boldsymbol{\gamma}}) \right]_{ii}}}, \quad i = 1, \ldots, a,$$

approaches a standard normal distribution if the proposed model is true, where $m_i(\boldsymbol{\theta} \mid \hat{\boldsymbol{\gamma}})$ is the ith element of the vector $\mathbf{m}(\boldsymbol{\theta} \mid \hat{\boldsymbol{\gamma}})$ and $[\mathbf{A}]_{ii}$ is the ith diagonal element of the $\mathbf{A}$ matrix. The

t_i statistic can be used to test the ith moment condition and its rejection implies a specification error with respect to the ith element in the $\boldsymbol{\gamma}$ vector of the auxiliary model.

The parameter estimates of the auxiliary model (29), together with the χ^2 statistics C and the corresponding EMM t_i statistics, are shown in Table 1. The EMM estimation results for the three continuous-time models are presented in Table 2. Two comments are called for. First, since the estimates of the δ_1 parameter in the SV model and in the SVJ model are both insignificant (see Table 2), we further estimate simplified versions of these two models that do not include the δ_1 parameter, which are also quite popular specifications in the literature. Second, since we use the same set of the auxiliary model in the projection step of the EMM estimation for all five continuous-time models, there is only one column of estimates for the parameter vector $\boldsymbol{\gamma}$ in the auxiliary model (the second column of Table 1). This can be contrasted to five columns of estimates for the parameter vector $\boldsymbol{\theta}$ (the last five columns of Table 2) as well as five columns of the EMM t_i statistics (the last five columns of Table 1), each corresponds to one of the five continuous-time models: two versions of the SV model (one with the δ_1 parameter and one without), two versions of the SVJ model, and the proposed SVF model.

From the second column of Table 1, we find the parameter estimates of the auxiliary AR(1)-EGARCH(1,1) model are all significant. In particular, the highly significant EGARCH coefficient estimates confirm the existence of the leverage effect; i.e., the effects of negative shocks z_t on h_{t+1} are larger than those of positive ones. Excess kurtosis in data does not seem to be adequately represented by the AR(1)-EGARCH(1,1) model and is left for the Hermite coefficients d_i to pick up so that the estimates of d_2, d_4, and d_8 are highly significant. Similar results have been reported by Anderson, Benzoni, and Lund (2002).

Let us move to the important question regarding which among the five estimated models can best describe the daily return data. In view of the large number of significant EMM t_i statistics and the enormous χ^2 statistics C in Table 1, we can immediately rule out the two versions of the SV model. As expected, the SVJ model substantially improves the empirical performance of its SV basis to the extent that the χ^2 statistics become insignificant even at the 95% level. Similar findings have been frequently reported in the literature. However, the SVJ model without the δ_1 parameter cannot fully accommodate excess kurtosis in the data so that the EMM t_i statistics corresponding to the d_4 and d_6 Hermite coefficients are significant. While adding the insignificant δ_1 parameter into the SVJ model helps alleviate this problem, the EMM t_i statistic for the b_2 (EGARCH) coefficient becomes moderately significant, indicating the persistency in volatility is not fully represented in this version of the SVJ model.

The SVF model proposed in this paper is by far the best model based on either the χ^2 statistics or the EMM t_i statistics. With the parameter number smaller than the full SVJ model, the SVF model can still attain a χ^2 statistic that is 17% smaller and ward off any significant EMM t_i statistic. It seems that the SVF model is able to characterize all the features of the conditional return distribution that have been captured by the semi-parametric auxiliary model.

Let us now turn to the parameter estimates of the continuous-time models given in Table 2. One salient feature in these results is the similarity in the estimates of those common parameters. For instance, the estimates of the $\delta_\circ$, δ_1, $\psi_\circ$, and ψ_1 parameters from the full versions of the SV

Table 1: The Estimates of the Auxiliary Model and the Corresponding t_i Statistics

	The Auxiliary Parameter	The EMM t_i Statistics				
		The SV Model		The SVJ Model		The SVF Model
$a_\circ$	0.0557* (0.0243)‡	−0.9680	−1.7397	−1.1777	−1.0839	−1.1802
a_1	0.0507** (0.0069)	1.3058	−0.8648	0.8648	−0.8719	−1.0028
$b_\circ^\dagger$	3.6319** (1.0323)	−1.3828	−1.8356	−0.6634	−1.7905	−1.0340
b_1	−0.1226** (0.0300)	1.5803	1.1494	0.3031	1.0824	1.0124
b_2	0.9355** (0.0023)	1.2436	1.9668*	0.5835	2.0797*	1.1536
c_1	−0.2861** (0.0696)	3.8054**	0.3523	0.5463	0.2137	−0.5284
c_2	0.2026** (0.0512)	1.5602	2.0386*	0.6085	1.7678	1.3835
d_1	−0.0727 (1.9938)	−3.1587**	0.5033	−0.9304	0.0338	0.6364
d_2	−1.2319** (0.1782)	−1.8336	1.8910	−1.6790	1.2433	1.0072
d_3	0.1311 (1.8676)	1.7984	−0.1193	0.6977	−0.7438	−0.2111
d_4	1.2884** (0.3568)	2.2976*	−0.8260	2.1892*	0.5953	0.6653
d_5	−0.1644 (1.8934)	−2.1706*	−0.0536	−0.4669	0.0509	−0.0434
d_6	−0.2609 (1.4373)	−2.8452**	−1.9912*	−2.6630**	−1.2748	−1.2122
d_7	0.1783 (2.3178)	−1.0202	0.0020	−0.5335	0.0370	0.0363
d_8	1.1894** (0.4356)	2.8078**	2.2157*	0.7094	1.4552	1.0008
χ^2 stat.		33.27**	32.74**	14.96	14.07	11.68
p-value		0.0002	0.0001	0.0599	0.0500	0.1661

† The $b_\circ$ coefficient estimate reported here is in fact $b_\circ/(1-b_2)$ using coefficient notation in the text. This minor reparameterization helps stabilize the numeric calculation.

‡ Numbers in parentheses are standard errors.

* denotes an estimate that is significant at 95% 1evel.

** denotes an estimate that is significant at 99% 1evel.

Table 2: The EMM Estimates of the Three Continuous-Time Models

Parameter	The SV Model		The SVJ Model		The SVF Model
Common Parameters:					
$\delta_\circ$	0.0364*	0.0246*	0.0296*	0.0221	0.0206**
	(0.0148)‡	(0.0151)	(0.0147)	(0.0117)	(0.0093)
δ_1		0.0149		0.0101	0.0109*
		(0.0187)		(0.0182)	(0.0053)
$\psi_\circ$	0.0078**	0.0070**	0.0139**	0.0069**	0.0057**
	(0.0023)	(0.0003)	(0.0027)	(0.0010)	(0.0006)
ψ_1	0.0146**	0.0131**	0.0175**	0.0124**	0.0140**
	(0.0045)	(0.0004)	(0.0035)	(0.0014)	(0.0040)
Parameters Specific to the SV and SVJ Models:					
σ	0.0728**	0.0702**	0.0698**	0.0686**	
	(0.0062)	(0.0050)	(0.0063)	(0.0061)	
ρ	−0.6003**	−0.6009**	−0.6102**	−0.6089**	
	(0.0430)	(0.0269)	(0.0466)	(0.0269)	
ζ			0.0202**	0.0202**	
			(0.0059)	(0.0047)	
φ			0.1346**	0.1329**	
			(0.0225)	(0.0308)	
Parameters Specific to the SVF Model:					
α					0.1206**
					(0.0012)
η					0.0475**
					(0.0135)
λ					1.4234**
					(0.1230)

‡Numbers in parentheses are standard errors.
* denotes an estimate that is significant at 95% 1evel.
** denotes an estimate that is significant at 99% 1evel.

and SVJ models are all fairly close to their counterparts in the SVF model. Based on this finding, we can conclude that the EMM estimation in general is quite stable. It is also interesting to point out that the SVJ model is unique in its jump intensity ζ parameter (i.e., the average number of jumps per day) of which the estimate 0.0202 implies approximately 5 jumps per year.

All the parameter estimates in the SVF model are decidedly significant, among which the most important one is the highly significant estimate 1.4234 of the volatility feedback effect λ. If we go back to equation (24) and check the magnitude of the depressing influence the volatility feedback effect λ imposes on return, we find that it is much stronger than the size of the trade-off δ_1 between risk and return, whose estimate is 0.0109, and the leverage effect η, whose estimate is merely 0.0475. In other words, the volatility feedback effect is not only statistically significant but also numerically dominant.

In comparison with other estimation procedures, the EMM estimation has the advantage that it allows us to *reproject* the unobserved state variable h_t.[15] As mentioned before, the state variable h_t in the SV model is the stock return volatility σ_{pt}^2 but not so in the SVF model. We can nevertheless follow (26) to compute the stock return volatility σ_{pt}^2 using the reprojected h_t from the SVF model. The stock return volatility for the SVJ model can also be computed in a similar way.[16] The resulting stock return volatilities for the entire sample period are shown in the bottom panel of Figure 1: those from the SVF model are in the upper half of that panel and results of the SVJ model (which are reprojected h_t themselves) are in the lower half. Although the changing patterns of reprojected stock return volatilities from both models are somewhat similar and generally match the movements in return data (shown in the upper panel of Figure 1), stock return volatilities from the SVF model are distinctively larger and much more fluctuating than those from the SVJ model. The sample average and standard deviation of reprojected stock return volatilities from the SVF model are, respectively, 1.4503 and 1.9822 and are larger than those of the SVJ model which are, respectively, 1.1358 and 0.6247.

We can also compute the covariance σ_{pht} between stock return and the change in the state variable h_t based on the reprojected h_t.[17] The results are shown in the middle panel in Figure

---

[15]After concluding the EMM estimation, we could get hold of 50,000 simulated data $\hat{y}_i(\hat{\boldsymbol{\theta}})$ and $\hat{h}_i(\hat{\boldsymbol{\theta}})$, $i = 1, 2, \ldots, 50,000$, generated from the estimated model; e.g., the SV, the SVJ, or the SVF model. We can use these simulated data to fit the auxiliary model in (29) and then calculate the predicted values of the volatility $\hat{s}_i^2(\hat{\boldsymbol{\theta}})$. With 50,000 sets of these values $\{\hat{y}_i(\hat{\boldsymbol{\theta}}),\ \hat{h}_i(\hat{\boldsymbol{\theta}}),\ \hat{s}_i^2(\hat{\boldsymbol{\theta}})\}$, we then fit a linear regression $\hat{h}_i(\hat{\boldsymbol{\theta}}) = \pi_\circ + \pi_1 \hat{s}_i^2(\hat{\boldsymbol{\theta}}) + \pi_2 \hat{y}_i(\hat{\boldsymbol{\theta}}) + \pi_3|\hat{y}_i(\hat{\boldsymbol{\theta}})| + e_t$. With the OLS estimates of the regression coefficients: $\tilde{\pi}_\circ$, $\tilde{\pi}_1$, $\tilde{\pi}_2$, and $\tilde{\pi}_3$, we then use real data y_t, $t = 1, 2, \ldots, T$, to calculate the fitted value of the unobserved state variable: $\tilde{h}_t = \tilde{\pi}_\circ + \tilde{\pi}_1 s_t^2 + \tilde{\pi}_2 y_t + \tilde{\pi}_3|y_t|$. The resulting fitted values $\tilde{h}_t$ are referred to as the *reprojected values* which can serve as estimates of the unobserved state variable h_t. See Gallant and Tauchen (2002) for more details.

[16]For the SVF model, σ_{pt}^2 is equal to $[(1 + 2\eta\lambda)^2 + 2\lambda^2 h_t]\, h_t$ according to (26). After we plug the parameter estimates into this formula, we get $\sigma_{pt}^2 = 1.2887\, h_t + 4.0521\, h_t^2$. For the SVJ model we have $\sigma_{pt}^2 = h_t + \zeta \cdot [\exp(\varphi^2) - 1] = h_t + 0.0004$.

[17]According to (28), σ_{pht} is equal to $-2\alpha[(1 + 2\eta\lambda)\eta + \lambda h_t]\, h_t = -0.0130\, h_t - 0.3433\, h_t^2$ for the SVF model. It is also readily shown that $\sigma_{pht} = \rho\sigma\sqrt{h_t^2 + \zeta \cdot [\exp(\varphi^2) - 1]\, h_t} = -0.0418\sqrt{h_t^2 + 0.0004\, h_t}$ for the SVJ model.

Figure 1

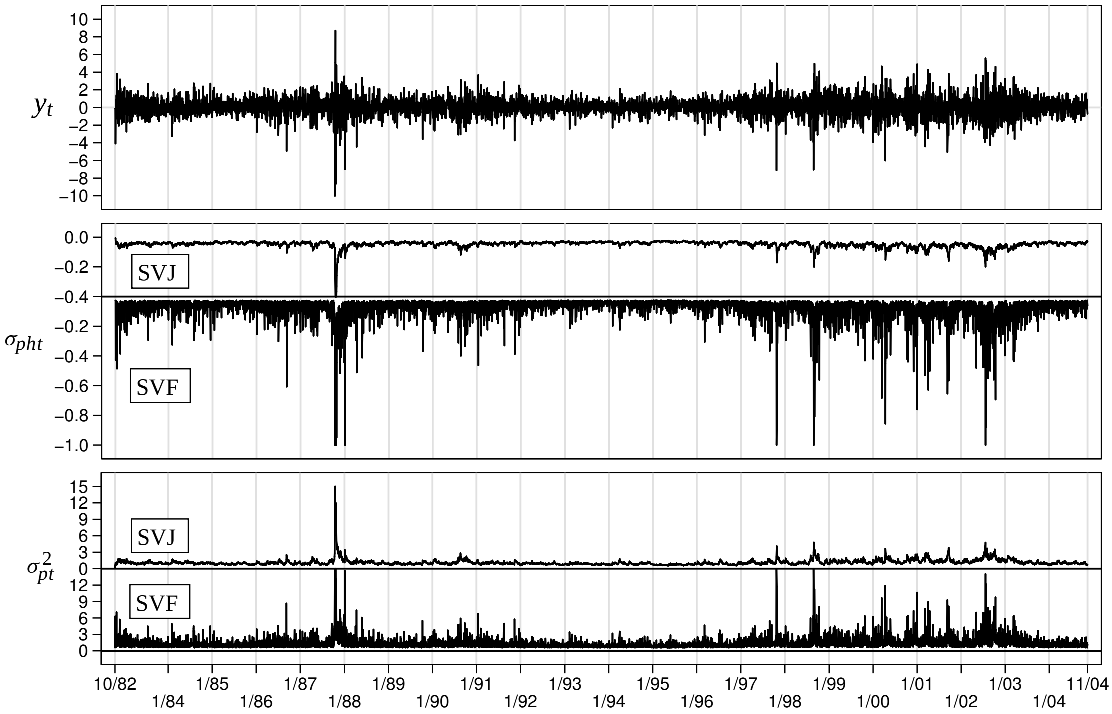

1. The patterns are similar to those of σ^2_{pt} while the contrast between the two models is even more pronounced. The sample average and standard deviation of the reprojected covariances from the SVF model are, respectively, -0.0813 and 0.1536 while those of the SVJ model are, respectively, -0.0475 and 0.0261 only.

These discussions seem to suggest that the proposed SVF model allows for much more empirical flexibility in σ^2_{pt} and σ_{pht} than the SVJ model. To further illustrate this point, we graphically show the dependence of the covariance σ_{pht} and the return variance σ^2_{pt} on the state variable h_t in Figure 2 (the two upper left panels) based on the estimated SVF and SVJ models. The range of h_t on the horizontal axis is between 0.25 and 1.5, which can be motivated by the reprojected values of h_t obtained from the SVF model. The sample average of these reprojected values of h_t from the SVF model is 0.4320, the sample median is 0.3821, and the standard deviation is 0.1841. The first, fifth, 95th, and 99 percentiles are, respectively, 0.2600, 0.2711, 0.7462, and 1.0732. The empirical distribution is severely skewed to the right. In particular, about 95% of the reprojected values of h_t are below 0.75. There are only 14 reprojected values of h_t that are outside the range $[0.25,\ 1.5]$.

In Figure 2 we find the variations of the covariance and variance from the SVF model (the solid curves) are much wider than those of the SVJ model (the long dash curves). It should be pointed out that this flexibility of the SVF model is resulted from the volatility feedback effect and will have important theoretical implications in the asset allocation problem as will be seen in the next section. In Figure 2 (again in the two upper left panels) we also draw the two curves (the short dash curves) for σ_{pht} and σ_{pt}^2 based on the SVF model with the volatility feedback coefficient λ suppressed to zero.[18] It is interesting to note that the resulting two curves are fairly close to those of the SVJ model (while the σ_{pt}^2 curves virtually overlap). The implication is that, so far as the asset allocation is concerned, the SVJ model might be as restrictive as the constrained version of the SVF model without the volatility feedback effect.

Figure 2

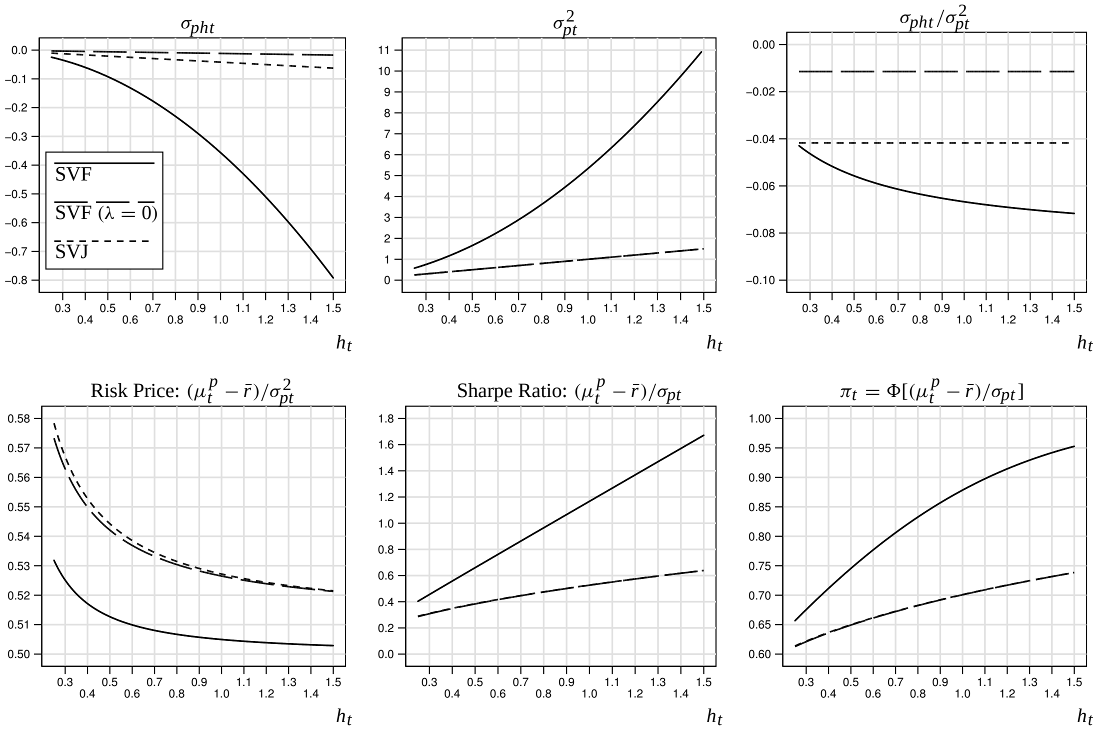

The last but not the least important issue is to check whether our continuous-time specification empirically is a good approximation to its discrete-time counterpart before we can apply Campbell and Hentschel's (1992) interpretations in terms of the volatility feedback effect. Hence, we should at least compare our parameter estimates with theirs. In this regard we should point out that Campbell and Hentschel used monthly return data in the 1980s to estimate their discrete-time model so that their estimation results might be different from ours which are based on daily data. With this potential discrepancy in mind, we find that, besides their estimate of the GARCH coefficient α is almost identical to ours, all other parameter estimates are reasonably close. On the one hand, their estimates of λ and η, 0.871 and 0.016 respectively,

[18] For the SVF model with $\lambda = 0$, we have $\sigma_{pht} = -2\alpha\eta\, h_t = -0.0115\, h_t$ and $\sigma_{pt}^2 = h_t$.

are smaller than ours, implying that both the volatility feedback effect and the leverage effect tend to diminish over a longer span of time. On the other hand, their estimate of the risk/return trade-off δ_1, which is 1.669, and mean-reverting speed of volatility ψ_1, which is 0.047, are larger than ours, a finding which can also be justified by the difference in data frequency. Based on the overall similarity in parameter estimates we thus conclude that our continuous-time SVF model is indeed a close approximation to the discrete-time version. Hence, all the interpretations generated from Campbell and Hentschel's (1992) theory of the stock return, particularly with respect to the volatility feedback effect, are applicable to our parameter estimates. This mapping provides us with a useful theoretical framework for further analysis on the strategic asset allocation problem.

4 Further Analysis of Asset Allocation

Once we determine which diffusion specifications (i.e., the SVF or the SVJ models suggested in the previous sections) to use, we can go back to the asset allocation analysis presented in Section 2 and assess the two terms ϕ^*_{Mt} and ϕ^*_{Ht} of the optimal investment weight in (9) not only qualitatively but also quantitatively.

It is important to note that the parameter estimates of the diffusion model can affect the optimal investment weight mainly through the risk price $(\delta_\circ + \delta_1 h_t - \bar{r})/\sigma^2_{pt}$ and the probability of earning excess return $\pi_t = \Phi[(\delta_\circ + \delta_1 h_t - \bar{r})/\sigma_{pt}]$ that depends on the Sharpe ratio $(\delta_\circ + \delta_1 h_t - \bar{r})/\sigma_{pt}$ in the myopic demand ϕ^*_{Mt} in (10) as well as the covariance-variance ratio $\sigma_{pht}/\sigma^2_{pt}$ in the intertemporal hedge demand ϕ^*_{Ht} in (11). It is therefore useful to examine how these terms depend on the state variable h_t in both the SVF and the SVJ models in Figure 2.[19]

Just like the earlier results regarding the curves for σ_{pht} and σ^2_{pt} (in the two panels in the upper left corner of Figure 2), the ranges spanned by the solid curves from the SVF model are much wider than the short dash curves from the SVJ model in every panel of Figure 2. We further draw those curves for the SVF model with the volatility feedback coefficient λ suppressed to zero and find that they are all quite similar to those of the SVJ model (the curves for Sharpe ratio and for π_t essentially overlap). From these graphical comparisons, we cannot but conclude once again that the restrictiveness of the SVJ model is about at the same level as the SVF model without the volatility feedback effect.

Based on the reprojected values of the state variable h_t from the SVF and the SVJ models that have been used to construct Figure 1, we compute the corresponding risk price, the probability π_t, and the covariance-variance ratio for all sample periods and present these time profiles in Figure 3. The return data are included again in the top panel as a reference.[20]

---

[19]Both the risk price and Sharpe ratio involve the drift term μ^p_t, i.e., $\delta_\circ + \delta_1 h_t$, of the dp_t/p_t process. Based on Ito Lemma, μ^p_t is equal to the drift term of the $dy_t = d\ln p_t$ process plus one half of the corresponding instantaneous variance σ^2_{pt}. The riskfree rate of return $\bar{r}$ is set at 0.005.

[20]Recall that for the the SVF model the risk price, the probability π_t, and the covariance-variance ratio are,

Figure 3

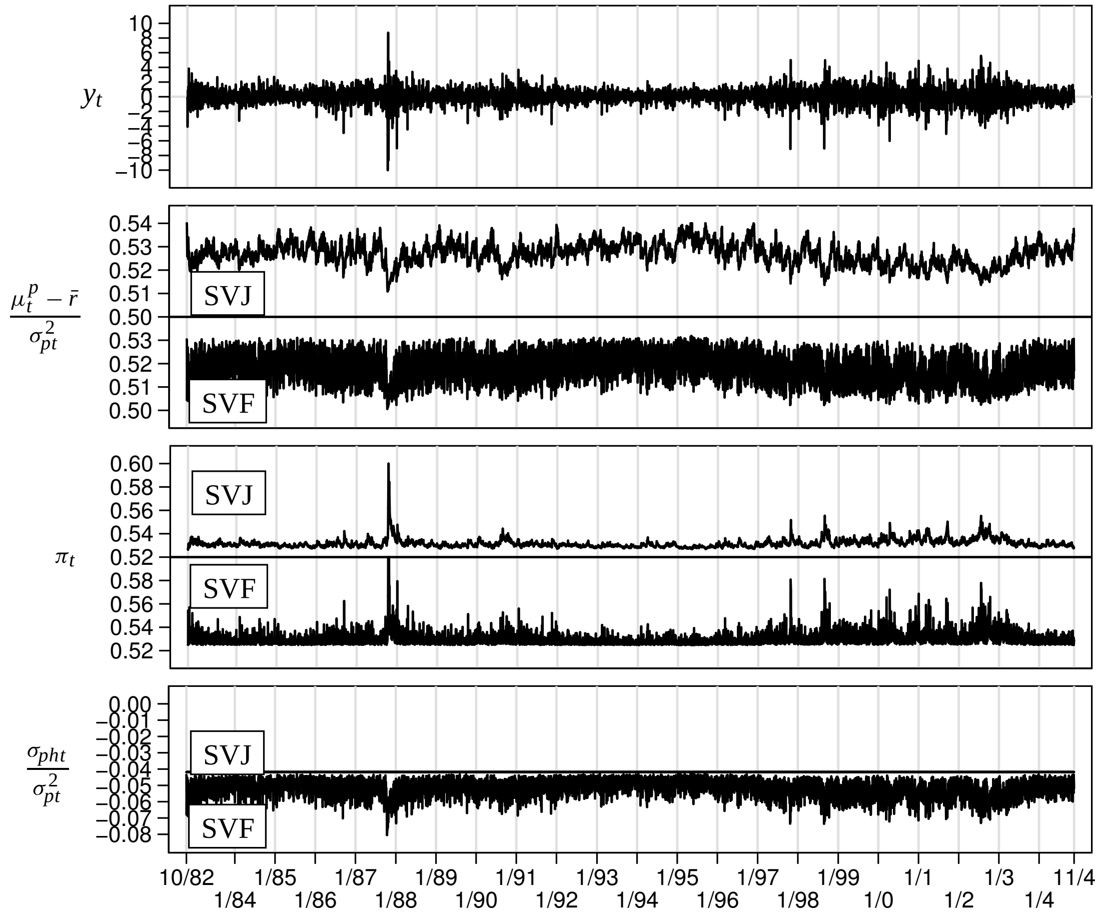

As expected, the time profiles of the reprojected risk price, the probability π_t, and the covariance-variance ratio are all much more variable in the SVF model than in the SVJ model. In particular, the covariance-variance ratio of the SVJ changes so little over the sample period that the corresponding curve essentially becomes a straight line (appearing in the middle of the bottom panel). It is therefore safe to infer that the SVF model and the theoretical interpretations associated with the volatility feedback effect can provide us with a sufficiently broad base to analyze both the myopic demand and the intertemporal hedge demand for the stock.

We have so far learned quite a lot about how parameter estimates of both the SVF and the SVJ models might affect asset allocation through the risk price, the probability π_t that depends

respectively, $(\delta_\circ+\delta_1 h_t-\bar{r})/\big[(1+2\eta\lambda)^2+2\lambda^2 h_t\big]h_t$, $\Phi\big\{(\delta_\circ+\delta_1 h_t-\bar{r})/\sqrt{[(1+2\eta\lambda)^2+2\lambda^2 h_t]h_t}\big\}$, and $-2\alpha\big[(1+2\eta\lambda)\eta+\lambda h_t\big]/[(1+2\eta\lambda)^2+2\lambda^2 h_t]$. The corresponding terms for the SVJ model are, respectively, $(\delta_\circ+\delta_1 h_t-\bar{r})/\big\{h_t+\zeta\cdot[\exp(\varphi^2)-1]\big\}$, $\Phi\big\{(\delta_\circ+\delta_1 h_t-\bar{r})/\sqrt{h_t+\zeta\cdot[\exp(\varphi^2)-1]}\big\}$, and $\rho\sqrt{h_t/\{h_t+\zeta\cdot[\exp(\varphi^2)-1]\}}$.

on Sharpe ratio, and the covariance/variance ratio. We are now ready to turn to the effects of preference parameters, i.e., the RRA coefficient γ, the narrow framing intensity coefficient $\nu_\circ$, and the loss aversion coefficient κ, on asset allocation.[21] Based on what we have observes in Figures 2 and 3, we will from now on focus on the SVF model and its special case with the volatility feedback coefficient λ set to zero in the analysis of asset allocation. This special case will be viewed as a proxy for the SVJ model.

4.1 The Myopic Demand for Stock

From (10) we know the RRA coefficient and the narrow framing/loss aversion parameters affect the myopic demand for stock respectively through two multiplicative factors: the reciprocal of the RRA coefficient and the n_t term. Most analysis in this subsection will be concentrated on the much more sophisticated n_t term which is generated by narrow framing/loss aversion. We mentioned earlier that the narrow framing parameter $\nu_\circ$ and the loss aversion coefficient κ actually have rather different effects on the n_t term although they must work together and therefore tend to be viewed as a joint concept. In this subsection we will make clear the distinction between narrow framing and loss aversion in an asset allocation framework.

We first note that, although the first two equalities in (15) imply that the n_t term is a linear function of, respectively, the narrow framing intensity coefficient $\nu_\circ$ and the loss aversion coefficient κ, this linear relationship is complicated by the time-varying probability π_t of earning excess return. More specifically, when κ is smaller than the odds $\pi_t/(1-\pi_t)$ of earning excess return, then $\nu_\circ$ and κ are substitute in the sense that a large $\nu_\circ$ needs to be paired with a small κ in order to hold n_t at a constant value. On the other hand, if κ is larger than the odds $\pi_t/(1-\pi_t)$, then $\nu_\circ$ and κ become complementary. This changeable relationship between $\nu_\circ$ and κ is best demonstrated by the contour curves in Figure 4, where the horizontal axis denotes the value of the κ coefficient whereas the vertical axis is for the $\nu_\circ$ coefficient. Each contour curve there consists of $\nu_\circ$ and κ combinations that yield the same n_t value (the attached label indicates the corresponding n_t value) and is defined by the functional form: $\nu_\circ = (1-n_t)/[(1-\pi_t)\cdot\kappa - \pi_t]$ for given values n_t and π_t. Here, the value of π_t, defined in (14), is based on the parameter estimates of the SVF model as well as a given value for h_t which is set to be 0.4320 – the sample average of the reprojected values of the state variable h_t generated from the SVF model. The resulting contour curves are drawn in the left panel of Figure 4. We further make contour curves with the volatility feedback coefficient λ set to zero (while all other parameters are still equal to the estimates from the SVF model) and present them in the right panel. As argued earlier (see Figure 2) these alternative results can be associated with the SVJ model and help us to assess the importance of the volatility feedback effect in asset allocation.

The most salient result in Figure 4 is that the pair of the contour curves associated with n_t and $2-n_t$ are symmetrical with respect to the vertical line at $\kappa = \pi_t/(1-\pi_t)$ (i.e., the odds of

[21]The subjective discounting factor τ is also a preference parameter. However, its effect on asset allocation is relatively minor and is ignored in most of our analysis.

Figure 4

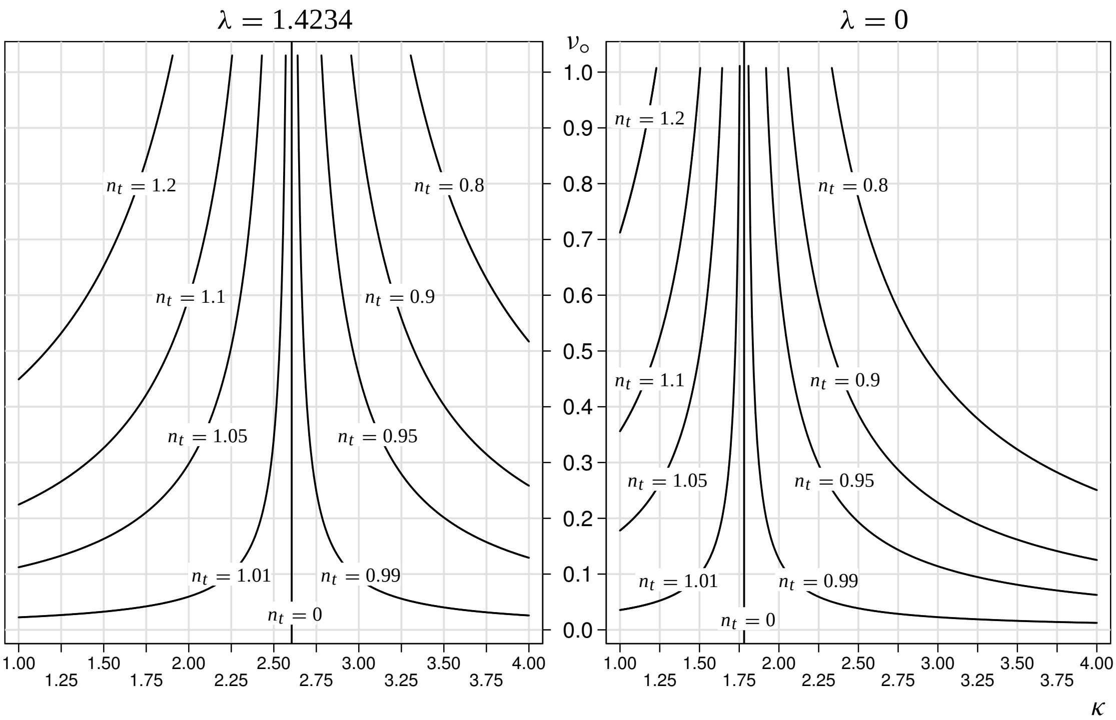

earning excess return which is equal to 2.605 in the left panel and is 1.781 in the right panel). When the loss aversion coefficient κ is a number smaller than $\pi_t/(1-\pi_t)$ in the left panel, say, 2, then increasing narrow framing intensity $\nu_\circ$ from 0 to 1 results in a greater n_t and therefore more myopic demand for stock. But if κ is a relatively large number like 3.5, then increasing narrow framing intensity $\nu_\circ$ from 0 to 1 will have opposite effects on myopic demand for stock. Similar patterns can also be found in the right panel. In contrast, if we fix the $\nu_\circ$ coefficient at any given value, then the n_t value will always decline as the κ value increases.

These findings are not surprising since they are nothing but the graphic presentation of the three equalities in (15). The importance of Figure 4 lies at the numerical relationship among n_t and the two parameters $\nu_\circ$ and κ, implied by each of the contour curves. For example, under the full SVF model, if the value of the narrow framing intensity $\nu_\circ$ is fixed at 0.65, then the myopic demand for stock will increase 20% in average as the loss aversion coefficient κ reduces from 2.6 to 1.5. More interesting, such an increase in the myopic demand can also be achieved by reducing the value of the narrow framing intensity $\nu_\circ$ from 0.8 to 0.18 while keeping the loss aversion coefficient κ at 3.5, or even by reducing the RRA coefficient from 3 to 2.5. Numerical comparisons like these give us a very concrete idea about the magnitude of the changes narrow framing/loss aversion can bring to asset allocation.

The difference between the two panels in Figure 4 quantitatively illustrates the effect of volatility feedback on the myopic demand for stock, from which we are able to assess the usefulness of the proposed SVF model in an asset allocation problem. For example, the loss aversion coefficient $\kappa = 1.781$ and the narrow framing intensity $\nu_\circ = 0.9$ together (which corresponding to a point on the contour curve labelled "$n_t = 1.2$" in the left panel) imply 20% increase in n_t as opposed to the case without narrow framing/loss aversion. But setting the volatility feedback effect to zero would completely erase such a gain in n_t.[22] The explanation for such changes is that the volatility feedback effect allows an investor of strong narrow framing (with $\nu_\circ = 0.9$) but weak loss aversion (with $\kappa = 1.781$) to develop an impression of favorable investment opportunity centering around the relatively large probability of earning excess return π_t. Such an investor will then try to capitalize this seemingly favorable investment opportunity by increasing the myopic demand for stock. However, if no volatility feedback effect is present, then the probability π_t will become less favorable in comparison with the degree of loss aversion κ so that the investor will cut back her myopic demand for stock.

Recall that both the probability π_t and the risk price under the SVJ model are close to those of the restricted SVF model without the volatility feedback effect (see Figure 2). As a result, we tend to think that the conclusion we draw from the restricted SVF model also holds under the SVJ model. But unfortunately it is not so because the return process of the SVJ model in (17) does not fit in the return process specification given in (1) so that the definition (10) of the myopic demand for stock is not applicable to the SVJ model. As a matter of fact, the SVJ model is not particularly useful for asset allocation analysis. See Liu, Longstaff, and Pan (2003) and Das and Uppal (2004).

Since the probability π_t is a function of the state variable h_t, we have to first pin down the probability π_t by setting h_t at a given value (for which we chose the sample average 0.4320 of the reprojected h_t from the SVF model) before we could use contour curves in Figure 4 to examine the relationship between the n_t term and the narrow framing/loss aversion parameters $\nu_\circ$ and κ. We can now go one step further to study how those contour curves are affected by the state variable h_t and how the myopic demand for stock, as a function of h_t, might be time-varying. We note that the horizontal coordinate $\pi_t/(1-\pi_t)$ of the straight vertical line in Figure 4 (which can be viewed as the center of the contour map) is an increasing function of π_t while we know from Figure 2 the probability π_t itself is also an increasing function of h_t. Consequently, all the contour curves will move horizontally to the right as the state variable h_t increases so that for any given combination of $\nu_\circ$ and κ the n_t term is an increasing function of h_t. This point can be made even more clear if we go back to (15) and note that the n_t term is a positively-sloped linear function of the probability π_t.

As to the relationship between the myopic demand for stock and the state variable h_t, we first present it graphically in Figure 5 for five cases of narrow framing/loss aversion, with and

[22] Setting the volatility feedback coefficient λ to zero also causes the risk price $(\mu_t^p - \bar{r})/\sigma_{pt}^2$ to rise from 0.5155 to 0.5470, which represents 6.1% increase (see the lower left panel in Figure 2) in the myopic demand for stock.

without the volatility feedback effect.[23] In the four cases with narrow framing/loss aversion (corresponding to the four dash curves among which the two black ones are for $\kappa = 3$ and the rest two gray ones are for $\kappa = 2$ whereas the long dash curves are for $\nu_\circ = 0.7$ and the short dash curves are for $\nu_\circ = 0.2$), the myopic demand for stock is an increasing function of h_t except at the very lower end of h_t.[24] This pattern simply reflects the fact that the myopic demand for stock is heavily dependent on the n_t term which in turn is a positively-sloped linear function of the probability π_t whose positive relationship with h_t is shown in Figure 2 (the lower right panel). To a large extent, the location and the slope of these curves are determined by the linear relationship between n_t and π_t as indicated in (15): $n_t = (1 - \nu_\circ \kappa) + \nu_\circ (1 + \kappa) \cdot \pi_t$. In other words, the height and the slope of the curves in Figure 5 are, respectively, proportional to $1 - \nu_\circ \kappa$ and $\nu_\circ (1 + \kappa)$.

Figure 5

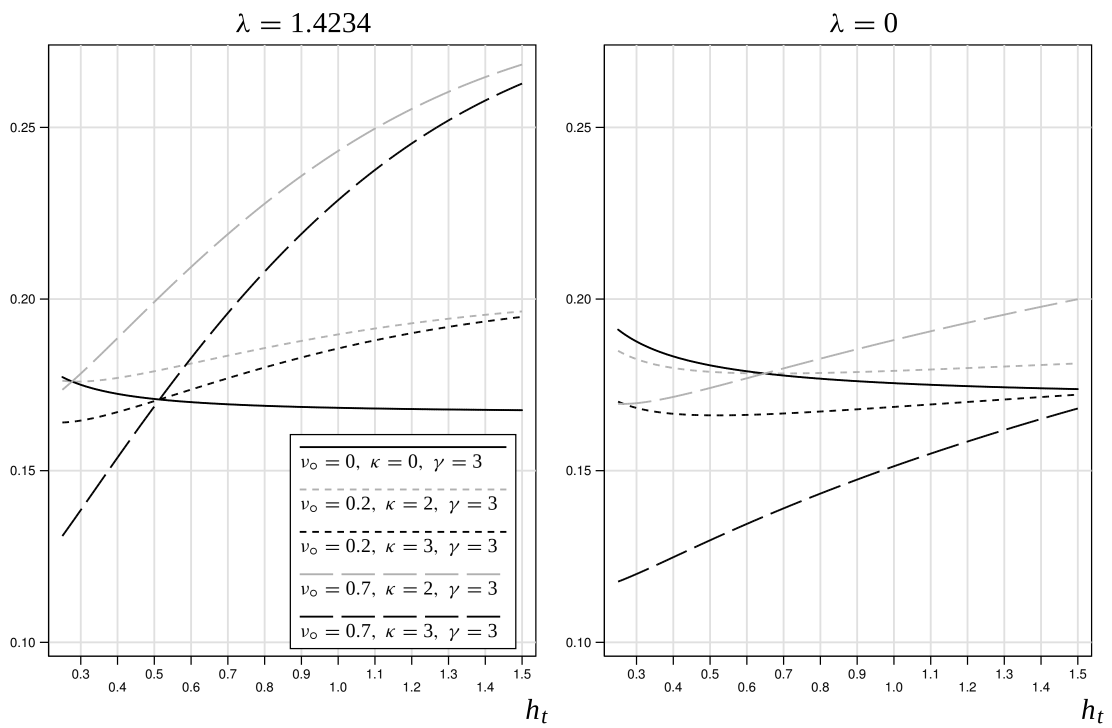

Let us now take a closer look at the left panel in Figure 5. We first note that the only

[23]When making the graphs, we assume the RRA coefficient γ is 3 while the specification of the risk price $(\mu_t^p - \bar{r})/\sigma_{pt}^2$ is identical to the one underlying Figure 2.

[24]The minor convex curvature at the lower end of h_t is due to the fact that the myopic demand for stock is not only a function of n_t but also proportional to the risk price $(\mu_t^p - \bar{r})/\sigma_{pt}^2$ while Figure 2 has shown that the risk price is a slowly decreasing function of h_t.

negative-sloped curve for the case without narrow framing/loss aversion (the solid curve) is exactly parallel[25] to the risk price curve in the lower left panel of Figure 2. Obviously, in the absence of narrow framing/loss aversion the myopic demand for stock will decline as volatility (i.e., the state variable h_t) increases, indicating the investor's typical response to increasing uncertainty. However, when narrow framing/loss aversion kicks in, the investor will start to view volatility from a different angle based on the probability π_t and sense that large volatility under the volatility feedback effect might mean an opportunity of earning excess return. When the chance of earning excess return becomes large enough to overcome her fear due to loss aversion, which tends to be true when volatility is sufficiently large, the investor will raise her demand for stock according to the factor $\nu_\circ(1 + \kappa)$. In other words, it is the volatility feedback effect that induces an investor with narrow framing/loss aversion to assess volatility from different viewpoints and then allocate assets with different proportions.

A comparison of the two panels in Figure 5 further highlights the marked effects of volatility feedback on the myopic demand for stock. While the negative-sloped curve for the case without narrow framing/loss aversion (the solid curve) in the right panel is higher than its counterpart in the left panel, the other four curves are all lower in the right panel and the difference indicates the size of the reduction in the myopic demand for stock we should expect once the inducement of earning excess return resulted from the volatility feedback effect disappears. We note that when the degree of loss aversion is large, i.e., when $\kappa = 3$, the reductions are particularly severe and the corresponding curves (the two black dash curves) lie completely below the curve for the case without narrow framing/loss aversion (the black curve). The explanation is that without the volatility feedback effect the odds of earning excess return simply cannot surpass the level of anxiety resulted from a large loss aversion coefficient 3 and the investor will reflexively cut back her demand for stock. It is also interesting to note that the four curves for the cases with narrow framing/loss aversion all have positive slopes, especially when the narrow framing parameter $\nu_\circ$ is large like 0.7. The cause for such positive relationships even in the absence of the volatility feedback effect is, interestingly, the leverage effect. We should point out that the way the leverage effect works on the myopic demand for stock is quite similar to the volatility feedback effect although the magnitude of its influence is much smaller.[26]

We have so far conducted a fairly thorough analysis of the relationship between narrow framing/loss aversion and the myopic demand for stock in which we have paid special attention to the role of the volatility feedback effect. As will become clear shortly, this relationship has profound impacts on every other aspects of the asset allocation problem. Here as a final remark, we note that the way the RRA coefficient γ affects the myopic demand for stock – as a reciprocal – is much simpler and is independent of the volatility feedback effect and narrow

[25]The proportionality factor is $1/\gamma = 1/3$.

[26]Recall that both the SV model and the SVJ model contain a parameter for the leverage effect. The present discussion gives us some ideas about how the myopic demand for stock might be affected by the leverage effect in those two models.

framing/loss aversion parameters. Hence, all the contour curves in Figure 4 are unaffected by γ while all the curves in Figure 5 will shift in a parallel fashion as γ changes – upward if γ decreases and downward if γ increases.

4.2 The Value Function and Consumption

Unlike the myopic demand, the derivation of the intertemporal hedge demand ϕ_{Ht}^* requires the knowledge of the $A(h_t, t)$ function and its partial derivative $A_h(h_t, t)$ with respect to h_t as indicated in (11). These functions can be solved for from the nonlinear partial differential equation (12) under the assumption that the stock return and its volatility follow the estimated SVF model with given values of the preference parameters γ, $\nu_\circ$, κ, τ as well as the terminal date T. We will present a fairly complete analysis of the $A(h_t, t)$ function in this subsection and then proceed with the study of the intertemporal hedge demand for stock in the next subsection.

Before solving the partial differential equation (12), let us first show some properties of the $A(h_t, t)$ function besides its association with the intertemporal hedge demand ϕ_{Ht}^*. As is clearly indicated in (7), the dependency of the value function $V(W_t, h_t, t)$ on the state variable h_t is through the $A(h_t, t)$ function while $V(W_t, h_t, t)$ is negatively related to $A(h_t, t)$ when $\gamma > 1$. Consequently, if the state variable h_t is correlated with stock returns and is able to characterize the changes in the investment opportunity set while the value function $V(W_t, h_t, t)$ represents the maximized utility the investor can achieve by exploiting the information in the state variable h_t, then $V(W_t, h_t, t)$ should be increasing in h_t and $A(h_t, t)$ is necessarily a decreasing function of h_t with a negative partial derivative $A_h(h_t, t)$ when $\gamma > 1$. From (8) we also find that the optimal consumption/wealth ratio $(C_t/W_t)^*$ is inversely related to the same $A(h_t, t)$ function. As a result, for $\gamma > 1$ there must exist a positive relationship, which is quite reasonable, between the value function $V(W_t, h_t, t)$ and the optimal consumption/wealth ratio $(C_t/W_t)^*$.

When solving the partial differential equation (12), we will set the subjective discounting factor τ at 0.01 and then consider two values, 3 and 5, of the RRA coefficient γ as well as two sets of values, (0.2, 2) and (0.7, 3), of the narrow framing/loss aversion parameters $(\nu_\circ, \kappa)$ to compare the impacts of different preference parameters on the $A(h_t, t)$ function. We will also examine the effects of different time horizons by considering two terminal date T — 6 months and 120 months (10 years).[27]

---

[27]We adopt the implicit finite difference method to solve the partial differential equation as in Brennan, Schwartz, and Lagnado (1998) and Xia (2001) did. We use the numerically stable Crank-Nicolson method to approximate the first- and second-order derivatives of $A(h_t, t)$. The value range of the state variable h_t is set to [0.05, 3] which is divided into 60 grids. Two time ranges, e.g., 6 months and 120 months, have been tried while each month is divided into 20 grids. Hence, we have $A(h_{t_j(i)}, t_j)$ for $h_{t_j(i)}$, $i = 1, 2, \ldots, 60$, as the values of the state variable h_{t_j} and t_j, $j = 1, 2, \ldots, N$ (= 120 and 2400), as the values of time. Given the values of $A(h_{t_{j+1}(i)}, t_{j+1})$ for all i but fixed j and a value of $\phi_{t_{j+1}}^*$, we can solve for $A(h_{t_j(i)}, t_j)$, for all i, and $\phi_{t_j}^*$ through iteration until both $A(h_{t_j(i)}, t_j)$ and $\phi_{t_j}^*$ converge. This process itself can be iterated from $j = N$ back to $j = 1$. Terminal conditions: $A(h_{t_N(i)}, t_N) = 1$, for all i, as mentioned in Theorem 1 are imposed to initiate the iteration. Furthermore, two Neumann-type boundary condition with respect to the value of h_{t_j} are imposed: $A_h(0.05, t_j) = 0$ and $A_h(3, t_j) = 0$, for each j.

Figure 6 presents the solution to $A(h_t, t)$ as a function of the state variable h_t. The left and the middle panels are for the cases with the terminal date T set at 120 months and 6 months, respectively, while the volatility feedback coefficient λ is set at 1.4234. The right panel is for the cases with λ suppressed to zero, in which the upper half is for the long horizon case with $T = 120$ months (referring to the vertical axis on the left edge) and the lower half is for $T = 6$ months (referring to the vertical axis on the right edge). Note that for the two long horizon cases (i.e., $T = 120$ months) the vertical coordinates should be multiplied by 10^4; e.g., 17.5 in the left panel stands for 175,000 while 70 in the upper half of the right panel means 700,000. Each panel contains three curves for the three specifications of the preference parameters $(\nu_\circ, \kappa, \gamma)$ which are $(0, 0, 3)$, $(0.2, 2, 3)$, and $(0.7, 3, 3)$, respectively, corresponding to the solid line, the gray short dash line, and the long dash line. The composition of the left panel is made slightly more complicated in order to present more information. Since $A(h_t, t)$ in this case has much wider variation when h_t is smaller than 0.6, we divide the three curves into two parts: the left part (the corresponding vertical axis is on the left edge and the horizontal axis on the top edge) is for h_t smaller than 0.6 while the right part (the corresponding vertical axis is on the right edge and the horizontal axis on the bottom edge) is for h_t greater than 0.6. The measurement unit along the vertical axis on the right is more than 4 times larger than the one on the right. Only in this format can we show more clearly how the three curves are related to each other, especially when h_t is greater than 0.6.

If we compare the left and the middle panels in Figure 6 for the case with $\lambda = 1.4234$, it is obvious that the three negative-sloped curves in both panels follow quite similar patterns: when h_t increases, the long dash curve (for $\nu_\circ = 0.7$ and $\kappa = 3$) lies above two other curves at the beginning, but it soon cuts the solid curve (for $\nu_\circ = 0$ and $\kappa = 0$) first and then the gray short dash one (for $\nu_\circ = 0.2$ and $\kappa = 2$) from above. The gray short dash curve is almost always below the solid one except at the very lower end. The relationship among three negative-sloped curves in the upper half of the right panel for the case with $\lambda = 0$ is also similar to that in the lower half: the long dash curve is always on the top while the gray short dash curve cuts the solid one from above. The most interesting feature of these patterns is that they are exactly symmetric to the patterns we found in the myopic demand for stock as shown in Figure 5.[28] Such symmetry reveals that the determination of the $A(h_t, t)$ function is greatly influenced by the myopic demand and the mechanism, as described in the previous subsection, that helps generate the myopic demand also works on the $A(h_t, t)$ function. An interesting corollary from this finding is that even though the two preference parameters $\nu_\circ$ and κ for narrow framing/loss aversion do not explicitly show up in the partial differential equation (12), they can greatly affect

[28] In the left panel of Figure 5 for the case with $\lambda = 1.4234$, when h_t increases, the black long dash curve (for $\nu_\circ = 0.7$ and $\kappa = 3$) lies below other curves at the beginning, but it soon cuts the black solid curve (for $\nu_\circ = 0$ and $\kappa = 0$) first and then the gray short dash one (for $\nu_\circ = 0.2$ and $\kappa = 2$) from below. The gray short dash curve is almost always above the black solid one except at the very lower end. In the right panel Figure 5 for the case with $\lambda = 0$, the black long dash curve is always on the bottom while the gray short dash curve cuts the black solid one from below. These patterns are like stretched mirror images of those in Figure 6.

Figure 6

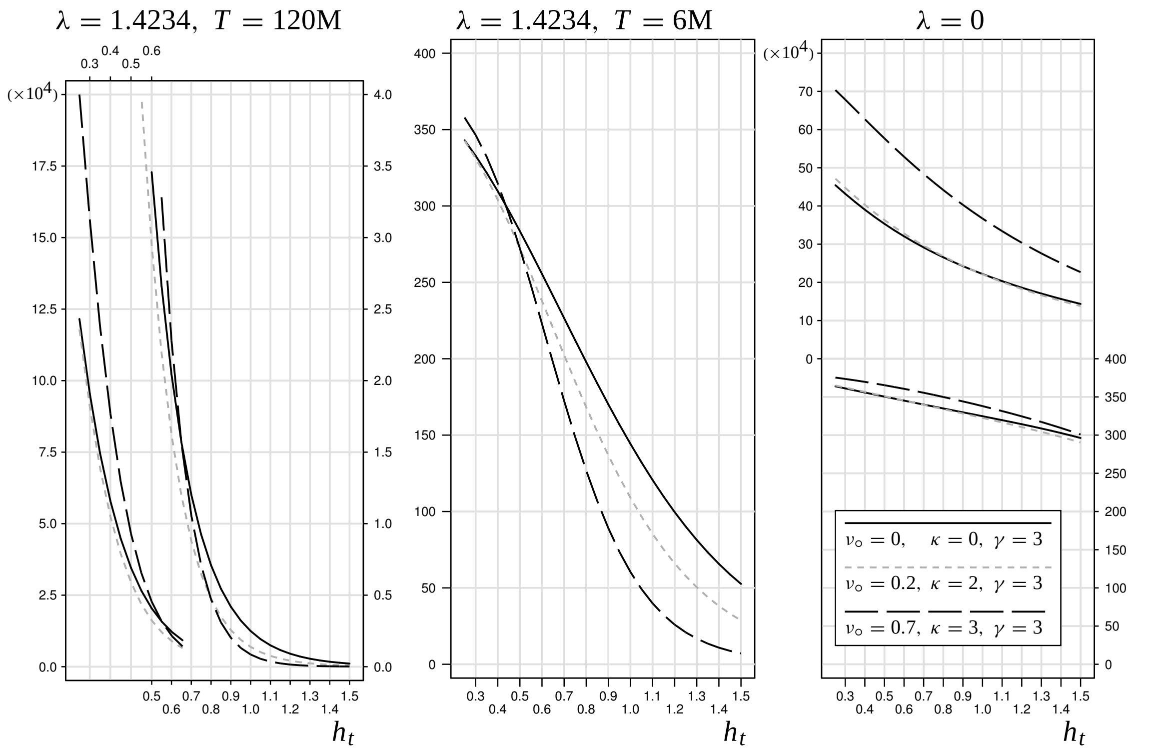

the dynamics of the $A(h_t, t)$ function (and therefore the intertemporal hedge demand for stock, the value function, and consumption) through their rather static effects on the myopic demand.

Let us now compare the three panels of Figure 6 more closely to examine the volatility feedback effect on the $A(h_t, t)$ function. We start with the long time horizon case with $T = 120$ months. We note that the three curves under the volatility feedback effect (in the left panel) begin at values about a quarter of and end at values only a hundredth of the corresponding values in the case without the volatility feedback effect (in the upper half of the right panel). Since the value function, or the maximum utility the investor can achieve, is negatively related to the $A(h_t, t)$ function, the above observation has the following interesting implications: When the volatility feedback effect is present and the time horizon is long enough for the investor to take advantage of it (referring to the left panel of Figure 6), the investor is able to not only achieve a much higher utility level but also elevate utility much more rapidly as the state variable h_t increases than in the case without the volatility feedback effect (referring to the upper half of the right panel). In fact as soon as h_t passes 1.0, the utility is already quite close to its maximum level when the volatility feedback effect is present. If we turn to the short time horizon case (with $T = 6$ months) and compare the middle panel with the lower half of the right panel, then we can infer that when the state variable h_t is at lower level, the utility level is about the same no matter whether the volatility feedback effect is present or not (this is different from the long time horizon case). But as h_t rises, the volatility feedback effect can help the investor to raise her utility at a much faster speed (this part is similar to the long time horizon case). Our conclusion from the above analysis is that the state variable h_t always helps enhance utility while the welfare increase is much larger under the volatility feedback effect and is particularly so if the time horizon is sufficiently long.

Another interesting result in Figure 6 is that the range of the $A(h_t, t)$ function in the long time horizon case, which can be as large as 700,000, is much greater than in the short time horizon case, which is less than 400. It seems counterintuitive at the first glance that the corresponding utility levels the investor can obtain are much larger in the short time horizon cases than in the long time horizon cases. The explanation is as follows: apart from the narrow framing/loss aversion factor in the utility function (3), it is consumption that generates utility. Given a fixed level of current wealth, the investor tends to consume more and therefore attains a higher utility level over the short time horizon than over the long time horizon if all the wealth is to be consumed at the terminal date as has been assumed in this paper. To further validate this argument, we use (8) to compute the optimal consumption/wealth ratio for the various cases in Figure 6 and show the results graphically in figure 7. The left and the middle panels are structured to illustrate more clearly the relationship among the curves for $h_t \leq 0.8$, just like in the left panel of Figure 6.

Figure 7

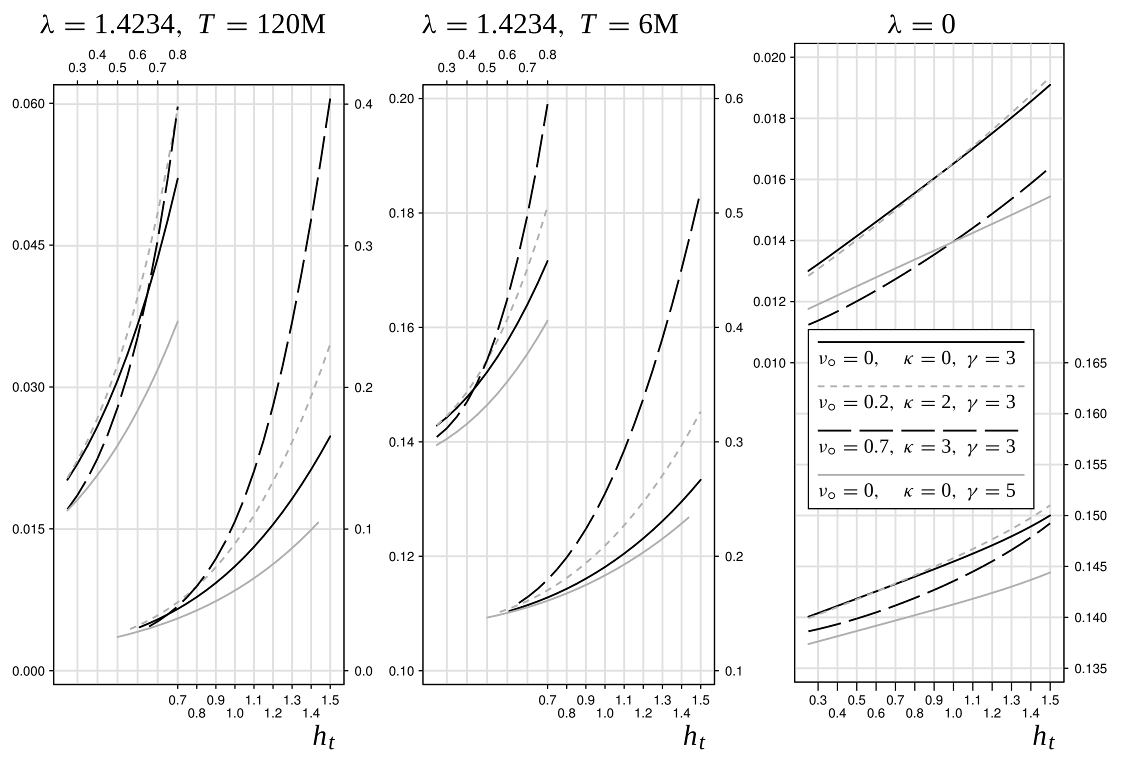

Figure 7 unequivocally confirms that the optimal consumption/wealth ratio is indeed much smaller in the long time horizon cases than in the short time horizon cases, especially when the state variable h_t is smaller than 0.8 (which accounts for more than 96% of reprojected observations reported in Subsection 3.3). For example, if the volatility feedback effect is present, the optimal consumption/wealth ratio is between 1.5% and 6% in the long time horizon case when h_t is smaller than 0.8, but is between 14% and 20% in the short time horizon case. Figure 7 contains many other interesting results (including the gray solid curve for the case with a larger RRA coefficient $\gamma = 5$) which will be further elaborated after we discuss the intertemporal hedge demand in the next subsection.

4.3 The Intertemporal Hedge Demand for Stock

Given the solutions to the $A(h_t, t)$ function, which is shown in Figure 6, and the accompanied partial derivative $A_h(h_t, t)$ with respect to the state variable h_t, we are ready to calculate the intertemporal hedge demand for stock based on its definition (11). The results as functions of h_t are shown in Figure 8: those with the volatility feedback effect are given in the left panel and those without are in the right panel. In each panel the upper two third, referring to the vertical axis on the left edge, is for the long time horizon case with the terminal date $T = 120$ months, while the lower one third, referring to the vertical axis on the right edge, is for the short time horizon case with the terminal date $T = 6$ months. Similar to Figure 7, four specifications of preference parameters are considered: the black solid curve is for the benchmark case where the RRA coefficient is 3 and narrow framing/loss aversion is not included; the two dash curves are for the same RRA coefficient but two different sets of narrow framing/loss aversion parameters; and the gray solid curve is for the case of a larger RRA coefficient $\gamma = 5$ and no narrow framing/loss aversion.

The immediate conclusion we can draw from Figure 8 is that the intertemproal hedge demand for stock is much larger when the volatility feedback effect is present or when the time horizon is long. In fact, in comparison with the corresponding myopic demand in the right panel of Figure 5 (whose magnitude is between 12% and 20%), the resulting intertemproal hedge demand for the case without the volatility feedback effect is way too small (less than 0.4%) to have any meaningful explanation. This finding is consistent with our earlier analysis on the covariance/variance ratio $\sigma_{pht}/\sigma_{pt}^2$ associated with Figure 2 (more specifically, the upper right panel) and on the consumption associated with Figure 7, namely, a larger value of the state variable h_t (the fundamental volatility) implies a greater opportunity for future returns under the volatility feedback effect and a longer time horizon stipulates less consumptions but more savings and investment. Based on the same reasons, it is also not surprising to find that all the curves in the left panel have positive slopes when h_t is smaller than 1.0.

What is surprising in the left panel of Figure 8 is that the two dash curves for the cases with narrow framing/loss aversion are consistently higher than the black solid curves and that at least three curves in the upper half for the case of long time horizon ($T = 120$ months) show a negative relationship with the state variable h_t when h_t becomes larger than 1.0. These findings

Figure 8

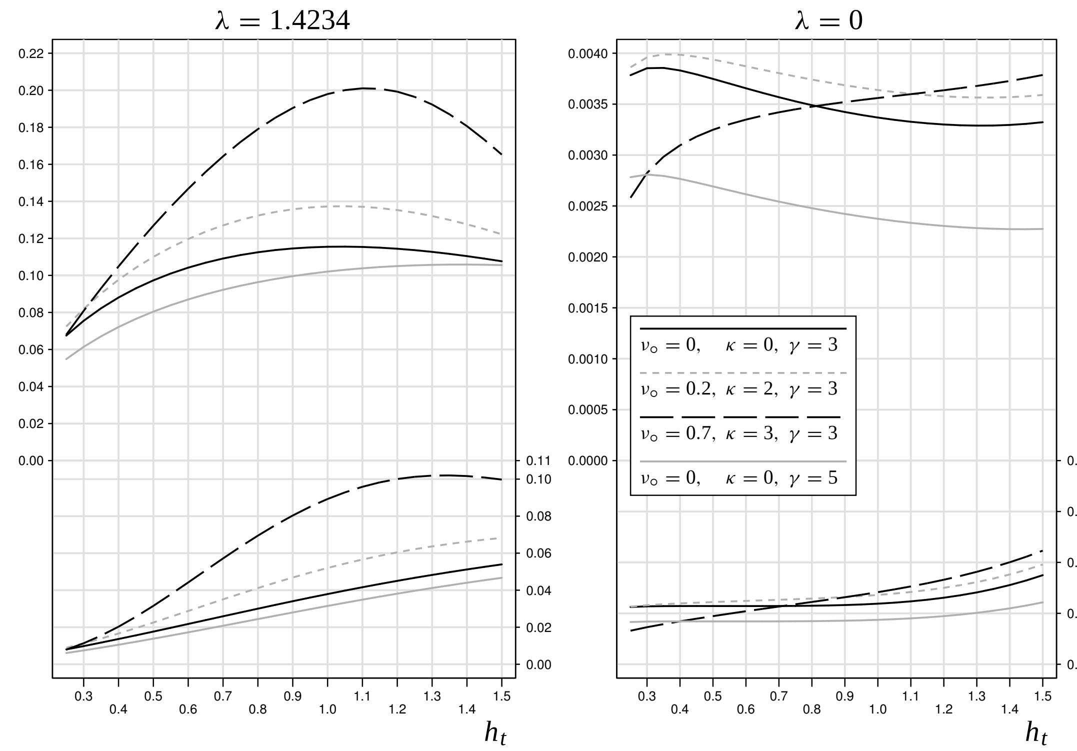

are in sharp contrast with the gray solid curve for the case with a larger RRA coefficient γ $(= 5)$ that is consistently lower than all other curves and is increasing in h_t. The behavior of the gray solid curve is what we would expect from an investor with strong risk aversion. But why does the investor with narrow framing/loss aversion desire so much intertemproal hedge demand for stock and why does such demand ever experience a negative relationship with the state variable h_t? The answer lies at the term A_h/A in the formula (11) of intertemproal hedge demand, which is closely related to the shape of the $A(h_t, t)$ function presented in the left and the middle panels of Figure 6. The two dash curves for the cases with narrow framing/loss aversion in the left and the middle panels of Figure 6 appear to to be steeper than the solid curve for any given value of h_t so that the absolute value of A_h/A tend to be larger when narrow framing/loss aversion is present.[29] An intuitive explanation for this particular relationship among the three curves in Figure 6 is that including narrow framing/loss aversion into the utility function given

[29]The gray short dash curve in either the left or the middle panel of Figure 6 is consistently lower than the solid curve, implying that the value of the $A(h_t, t)$ function corresponding to the former curve is consistently smaller. This feature helps raise the absolute value of A_h/A. As for the black long dash curve, although it is higher than the solid curve for smaller h_t, its slope in absolute value appears to be substantially larger than that of the solid curve so that the absolute value of A_h/A remains larger for all values of h_t.

in (3) means adding into the value function of $V(W_t, h_t, t)$ an additional term that is responsive to changing h_t. This additional term helps enhance the sensitivity of the value function and therefore the $A(h_t, t)$ function with respect to h_t. At this conjunction we should point out that while the slope of the $A(h_t, t)$ function, or the investor's sensitivity toward the state variable h_t, plays a major role in determining the investor's intertemporal hedge demand, it is the magnitude of the $A(h_t, t)$ function that reflects how the investor decides the myopic demand for stock as mentioned earlier.

Since the curves in the left and the middle panels of Figure 6 are quite steep, especially the black long dash curve in the left panel for the case with strong narrow framing/loss aversion and long time horizon, the corresponding $A(h_t, t)$ functions tend to rapidly reach their respective minima with the partial derivative A_h simultaneously converging to zero as h_t increases. Consequently, it is not possible for the intertemporal hedge demand for stock to remain increasing in h_t for too long and the corresponding curves shown in the left panel of Figure 8 will have to turn back down as h_t increases. Once again, it is the investor's sensitivity toward the state variable h_t that stipulates such a pattern of the intertemporal hedge demand for stock. A possible intuition is that the opportunity of earning more future returns opened up by increasingly larger state variable h_t through the volatility feedback effect simply cannot be expanded forever. The investor will eventually respond to accompanied declining risk prices and adjust the intertemporal hedge demand accordingly. It is also worthwhile to point out that the peculiar behavior of the intertemporal hedge demand for stock under narrow framing/loss aversion reminds us of its pronounced dynamic effects in addition to its dominant role in the myopic demand, although the n_t term does not explicitly show up in the definition (11) of the intertemporal hedge demand or even in the partial differential equation (12).

4.4 Investment, Consumption and Savings

At each period of time the investor divides her wealth into tree parts for, respectively, consumption, investment to stock, and savings, where savings can also be viewed as investment to the riskless asset with a fixed rate of return $\bar{r}$. By summing up the myopic demand and the intertemporal hedge demand for stock, we obtain the investment weight ratio. Subtracting this ratio and the consumptio/wealth ratio (computed in Subsection 4.2) from one, we get the savings/wealth ratio. The results of these three ratios are shown in Figure 9, in which the consumptio/wealth ratio is reproduced from Figure 7 for easy reference. The three upper panels of Figure 9 are for the case with the volatility feedback effect and the three lower panels are for the alternative case. The definitions of the four curves in each panel are exactly the same as those in Figure 7 and the legend is omitted to save space. Inside each panel the upper half (corresponding to the vertical axis on the left edge) is for the long time horizon case with $T = 120$ months while the lower half (corresponding to the vertical axis on the right edge) is for the short time horizon case with $T = 6$ months

From Figure 9 we find that increasing the narrow framing/loss aversion parameters tends to strengthen the three ratios' responsiveness to the state variable h_t and therefore rotate the

Figure 9

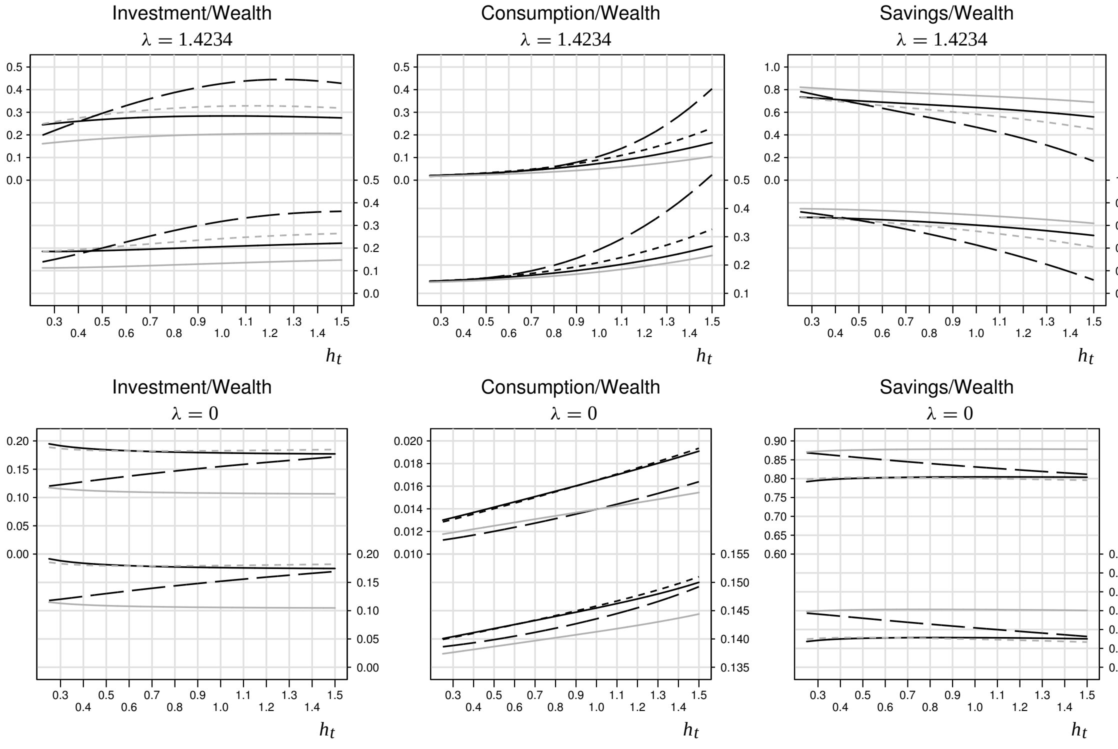

three curves away from the horizontal line (particularly when the volatility feedback effect is present), while increasing the RRA coefficient γ tends to shift all the ratios in a parallel fashion. By comparing the two right panels of Figure 9 with Figure 5 and Figure 8, it is readily seen that, irrespective of the length of time horizon, the investment weight ratio is a mixture of the myopic demand and the intertemporal hedge demand for stock so that it shares the features of both types of demand when the volatility feedback effect is present. If the volatility feedback effect is absent, then the investment weight is virtually identical to the myopic demand so that the investment weight remains about the same over both time horizons.

4.5 Summary Statistics

The previous four subsections respectively present theoretical partial analysis of how the myopic demand and the intertemporal hedge demand for the risky asset as well as consumption, savings, and the welfare, respectively, respond to changes in the state variable h_t, the volatility feedback effect λ, narrow framing/loss aversion parameters $\nu_\circ$ and κ, the RRA coefficient γ, and the time horizons T. The effects of the state variable h_t are particularly emphasized. In this subsection we shall present a more general picture about our empirical results by analyzing sample means and sample standard deviations for investment, consumption, and savings of the

5572 daily data that we employ to estimate the proposed SVF model.

Recall that earlier in Figures 1 and 3 we used the reprojected h_t, $t = 1, 2, \ldots, 5572$, for all sample periods to compute the corresponding estimates for σ_{pht}, σ^2_{pt}, etc. Now, given 16 different specifications of the volatility feedback effect λ, narrow framing/loss aversion parameters $\nu_\circ$ and κ, the RRA coefficient γ, and the time horizons T, we can also compute the estimates for the optimal portfolio weights ϕ^*_{Mt} (the myopic demand for stock), ϕ^*_{Ht} (the intertemporal demand for stock), and ϕ^*_t (the total demand for stock), the optimal consumption-wealth ratio $(C_t/W_t)^*$, and the savings-wealth ratios for all sample periods t. In Tables 4 and 5 we show the sample means and standard deviations of all these results.

Table 4: The Sample Means of the Asset Allocation

T	γ	$\nu_\circ$	κ	Myopic Demand	Hedge Demand	Invest.	Consump.	Savings
				$\lambda = 1.4234$				
120	3	0	0	0.1722	0.0904	0.2626	0.0297	0.7076
	3	0.2	2	0.1784	0.1013	0.2797	0.0317	0.6887
	3	0.7	3	0.1608	0.1139	0.2747	0.0286	0.6968
	5	0	0	0.1033	0.0747	0.1780	0.0231	0.7989
6	3	0	0	0.1722	0.0159	0.1881	0.1513	0.6606
	3	0.2	2	0.1784	0.0200	0.1984	0.1536	0.6480
	3	0.7	3	0.1608	0.0272	0.1880	0.1552	0.6567
	5	0	0	0.1033	0.0124	0.1158	0.1458	0.7384
				$\lambda = 0$				
120	3	0	0	0.1829	0.0038	0.1866	0.0139	0.7994
	3	0.2	2	0.1801	0.0039	0.1840	0.0138	0.8022
	3	0.7	3	0.1273	0.0031	0.1304	0.0119	0.8577
	5	0	0	0.1097	0.0027	0.1124	0.0124	0.8752
6	3	0	0	0.1829	0.0006	0.1834	0.1415	0.6751
	3	0.2	2	0.1801	0.0006	0.1807	0.1414	0.6779
	3	0.7	3	0.1273	0.0004	0.1277	0.1397	0.7326
	5	0	0	0.1097	0.0004	0.1101	0.1384	0.7514

From Table 4 we find that the intertemporal hedge demands for stock are all smaller than the myopic demands and are particularly so in those cases with $\lambda = 0$. This last finding is consistent with what Liu (2001) has concluded from the SV model, which is more or less equivalent to the cases with $\lambda = 0$, that the intertemporal hedge demand tends to be substantially small in comparison with the myopic demand irrespective the status of the state variable.

The savings occupy the largest portion of the wealth and their ratios appear fairly stable across various cases. In contrast, consumption is almost always the smallest but can change substantially over different time horizons. In fact, shortening time horizon causes considerably more consumption and its funding can come either from investment or from savings, depending on whether the volatility feedback effects are present or not. Such horizon effects on investment (the investor tends to acquire a larger investment weight over a longer time horizon) work only through the hedge demand and is noteworthy only when the volatility feedback effects are present. Moreover, neither narrow framing/loss aversion nor risk aversion affect the magnitude of the horizon effect in any discernible manner. It is important to point out that all these results are nothing but reflections of the patterns we found earlier in Figure 9 corresponding to the value 0.4320 of h_t which is the sample average of the reprojected h_t.

4.5.1 The Equity Premium Puzzle

Irrespective of the length of time horizon, narrow framing/loss aversion helps reduce investment and transfer the weights largely to savings so long as the volatility feedback effects are suppressed to zero. For example, from Table 4 we find that when the time horizon is 120 months and the RRA coefficient γ is 3, then changing the values of narrow framing/loss aversion parameters $(\nu_\circ, \kappa)$ from (0, 0) to (0.7, 3) shrinks the investment weight from 18.66% to 13.04%. This result seems to confirm that narrow framing/loss aversion can explain the equity premium puzzle that the investor tend to invest less in stocks than what the standard asset allocation theory suggests. In this regard we note that Berkelaar, Kouwenberg, and Post (2004) and Gomes (2005) refer to this phenomenon of reducing the portfolio weight of stocks as a partial portfolio insurance strategy in their analyses of loss aversion. However, when we introduce the volatility feedback effect into the analysis, then the direction of the weight shifts actually reverses: the investment weight increases slightly from 26.26% to 27.47%. This observation may very well be the most interesting finding in Table 4 regarding the interactions between narrow framing/loss aversion and the volatility feedback effect: how narrow framing/loss aversion affects the proportion of investment on the risky asset and on the riskless asset (i.e., savings) depends crucially on whether the volatility feedback effect is considered or not. To put it more precisely, narrow framing/loss aversion probably cannot explain the equity premium puzzle on average if the investor is perceptive of the information in the state variable and can take advantage of the investment opportunities opened up by the volatility feedback effects.

4.5.2 Risk Aversion vs. Loss Aversion

It is perhaps not surprising to find in Table 4 that increasing RRA coefficient γ from 3 to 5 (meaning higher degree of risk aversion) causes a reduction in the investment in every case. What is surprising is the size of such a reduction which is much larger than the changes caused by narrow framing/loss aversion, especially in the myopic part of the investment. Three comments are called for.

First of all, we should not read too much of this result and hastily conclude that the traditional risk aversion plays a much more important role in a dynamic asset allocation problem than narrow framing/loss aversion does. To see why it is so let us turn to Table 5. The most distinctive pattern in Table 5 is those considerably large standard deviations in investment, consumption, and savings associated with narrow framing/loss aversion when the volatility feedback effect is present. Because the sample variations behind the standard deviations in Table 5 are all set off by the time-varying state variable h_t, the investor under narrow framing/loss aversion is definitely more sensitive to the information in the state variable through the volatility feedback effects. In other words, the effects of narrow framing/loss aversion on asset allocation are more of the dynamic nature than the effects of risk aversion. It is then difficulty to argue which of loss aversion and risk aversion is more important since they simply exert their influences through different channels.

Secondly, we should also point out that large standard deviations in investment proportions under narrow framing/loss aversion and under the volatility feedback effects imply excessive trading volume in the market of the risky asset. In other words, the loss averse investor tends to switch her investment between the risky asset and the riskfree asset much more frequently by gathering information in the state variable more closely. This result is consistent with Gomes' (2005) finding about trading volume.

Table 5: The Standard Deviations of the Asset Allocation

T	γ	$\nu_\circ$	κ	Myopic Demand	Hedge Demand	Invest.	Consump.	Savings
					$\lambda = 1.4234$			
120	3	0	0	0.0019	0.0113	0.0094	0.0115	0.0197
	3	0.2	2	0.0031	0.0152	0.0181	0.0151	0.0315
	3	0.7	3	0.0214	0.0292	0.0505	0.0216	0.0678
	5	0	0	0.0012	0.0107	0.0095	0.0070	0.0160
6	3	0	0	0.0019	0.0064	0.0047	0.0102	0.0148
	3	0.2	2	0.0031	0.0093	0.0124	0.0143	0.0262
	3	0.7	3	0.0214	0.0177	0.0390	0.0255	0.0621
	5	0	0	0.0012	0.0054	0.0044	0.0077	0.0121
					$\lambda = 0$			
120	3	0	0	0.0034	1.1×10^{-4}	0.0035	0.0007	0.0028
	3	0.2	2	0.0014	0.8×10^{-4}	0.0015	0.0008	0.0010
	3	0.7	3	0.0073	2.0×10^{-4}	0.0075	0.0006	0.0081
	5	0	0	0.0020	1.0×10^{-4}	0.0021	0.0005	0.0017
6	3	0	0	0.0034	1.1×10^{-5}	0.0034	0.0012	0.0023
	3	0.2	2	0.0014	2.5×10^{-5}	0.0014	0.0013	0.0011
	3	0.7	3	0.0073	8.1×10^{-5}	0.0074	0.0010	0.0084
	5	0	0	0.0020	0.7×10^{-5}	0.0020	0.0008	0.0013

Finally, it is worthwhile to note that Berkelaar, Kouwenberg, and Post (2004) and Gomes (2005) claim they cannot empirically disentangle loss aversion from risk aversion because both are confounded with each other in their utility specification. They therefore conclude that risk aversion and loss aversion are substitutes. The reason that we are able to separate loss aversion from risk aversion is because that loss aversion is an additive term in the utility function under narrow framing and in such a framework risk aversion and loss aversion are not necessarily substitutes for each.

5 Conclusion

We have conducted an in-depth analysis of the dynamic asset allocation problem over different time horizons in which the representative investor's preference includes narrow framing/loss aversion parameters while the intertemporal budget constraint contains the empirically validated volatility feedback effects. More precisely, the structure of narrow framing/loss aversion mechanism in the utility function is well-behaved enough to allows us express the solution to the dynamic asset allocation in an analytically tractable fashion. The optimal investment weight can be decomposed into two terms: one accounts for the myopic demand for investment and the other for intertemporal demand. One of the theoretical findings is that narrow framing/loss aversion parameters have much more direct and intelligible effects on the former than on the latter. These theoretical discussions have been presented in section 2.

To fully account for the intertemporal effects of narrow framing/loss aversion preferences, we are obliged to construct a flexible intertemporal budget constraint which reveals not only the behavior of an empirically plausible return process but also the dynamics of certain state variable. To this end, we propose in section 3 the stochastic volatility feedback model in which volatility serves as the state variable to allow for nonlinear time-vary investment opportunities for investor to hedge against. Our empirical results based on the efficient method moment estimation not only provide us with realistic parameter values for the return process but also show the proposed model is superior to popular stochastic volatility model and stochastic volatility with jump model.

Once we obtain parameter estimates for the intertemporal budget constraint, in section 4 we then conduct a detailed sensitivity analysis of the optimal allocation of the wealth among investment, consumption, and savings as well as the corresponding welfare level with respect to changes in various parameters including (1) preference parameters like narrow framing coefficient $\nu_{\circ}$, loss aversion coefficient κ, and risk aversion coefficient γ; (2) the terminal condition parameter; i.e., the length of time horizon T, as well as (3) one budget constraint parameter – the volatility feedback effect λ. More specifically, we divide the sensitivity analysis into two parts. In the first part we study how changes in various parameters affect optimal investment, consumption, savings, and welfare as functions of the state variable h_t. The results were reported in subsections 4.1 – 4.4. In the second part of the sensitivity analysis, the discussion is narrowed down to the optimal solution at the mean value of the state variable as shown in subsection 4.5.

The main findings regarding the sensitivity analysis of the myopic demand for stocks are as follows: When there is no narrow framing/loss aversion, this type of investment is a decreasing function of h_t and is roughly proportional to the risk price; i.e., $(\mu_t^p - \bar{r})/\sigma_{pt}^2$, implying an investor's typical response to uncertainty. However, when narrow framing/loss aversion is present, the myopic demand becomes increasing in h_t, proportional to the probability π_t of earning excess return, and is highly sensitive to the volatility feedback effect (as well as the leverage effect). As to the sensitivity analysis of the intertemporal hedge demand for stocks, we find that it is highly sensitive to h_t under narrow framing/loss aversion, and becomes much larger when the volatility feedback effect is present and/or when the time horizon is long. These findings all point to one conclusion that increasing the narrow framing/loss aversion parameters tends to strengthen the responsiveness of the investment with respect to the state variable h_t, which in turn necessitates similar patterns in the optimal levels of consumption and savings. It is interesting to note that increasing the risk aversion parameter γ does not have such effects and our analysis can separate the very different effects of risk aversion from those of loss aversion.

From the sensitivity analysis centering around the mean value of the state variable, we note that when the volatility feedback effect is absent, then narrow framing/loss aversion helps reduce investment and transfer the weights to savings. This result seems to suggest that narrow framing/loss aversion can explain the equity premium puzzle. However, we must point out that, when the volatility feedback effect kicks in, then the direction of the weight shifts reverses. The final verdict is that if the investor is perceptive of the information in the state variable and can take advantage of the investment opportunities opened up by the volatility feedback effects, then narrow framing/loss aversion alone probably cannot explain the equity premium puzzle.

Appendix 1: The Proof of Theorem 1

Before proving Theorem 1, we first present a useful lemma that is based on Ito-Tanaka formula (see, for example, Chung and Williams, 1990, and Klebaner, 1998):

Lemma 1 *a For any function g, define $\mathcal{D}^+ g(z) \equiv \lim_{\epsilon \to 0}[g(z+\epsilon) - g(z)]/h$, then for the loss aversion function K defined in Assumption 1, we have*

$$\mathcal{D}^+ K(z) = 1_{[0,\infty)}(z) - \kappa \cdot 1_{(-\infty,0)}(z),$$

where $1_A(z)$ equals 1 if $z \in A$, and equals 0 otherwise. Furthermore, given that $L(dt, x)$ is the local time of $(p_{t+dt} - p_t)/p_t - \bar{r}\,dt$ defined by

$$L(dt,x) \equiv \lim_{\epsilon \to 0} \frac{1}{2\epsilon} \int_t^{t+dt} 1_{(x-\epsilon, x+\epsilon)} \left[\frac{p_s - p_t}{p_t} - \bar{r}(s-t) \right] ds,$$

we have

$$\begin{aligned} & K\left(\frac{p_{t+dt} - p_t}{p_t} - \bar{r}\,dt \right) \\ &= K\left(\frac{p_t}{p_t} - 1 \right) + \int_t^{t+dt} \mathcal{D}^+ K \left[\frac{p_s - p_t}{p_t} - \bar{r}(s-t) \right] d\left[\frac{p_s - p_t}{p_t} - \bar{r}(s-t) \right] \\ &\qquad + \frac{1+\kappa}{2} \int_{-\infty}^{\infty} L(dt,x) \cdot 1_{\{0\}}(x)\, dx \\ &= \int_t^{t+dt} \left\{ 1_{[0,\infty)} \left[\frac{p_s - p_t}{p_t} - \bar{r}(s-t) \right] - \kappa \cdot 1_{(-\infty,0)} \left[\frac{p_s - p_t}{p_t} - \bar{r}(s-t) \right] \right\} \\ &\qquad \times d\left[\frac{p_s - p_t}{p_t} - \bar{r}(s-t) \right] + \frac{1+\kappa}{2} L(dt, 0), \end{aligned}$$

where the first equality is due to Ito-Tanaka formula.

(Proof of Theorem 1)

Replacing the term $e^{-\tau\, dt}$ in (3) by the approximation $1 - \tau \cdot dt$ (cf. Uppal and Wang, 2003) and then dividing both sides of (3) by dt yield

$$\begin{aligned} \sup_{C_t, \phi_t} \Bigg\{ & \frac{C_t^{1-\gamma}}{1-\gamma} + \nu \cdot \mathrm{E}_t \left\{ \frac{1}{dt} K \left[\phi_t W_t \cdot \left(\frac{p_{t+dt} - p_t}{p_t} - \bar{r}\,dt \right) \right] \right\} - \tau \cdot \mathrm{E}_t(V_{t+dt}) \\ & + \frac{1}{dt} \Big[\mathrm{E}_t(V_{t+dt}) - V_t \Big] \Bigg\}. \end{aligned}$$

First, by the definition of differential generator we have

$$\lim_{dt \to 0} \frac{1}{dt} \Big[\mathrm{E}_t(V_{t+dt}) - V_t \Big] = \nabla V_t.$$

Secondly, given $\phi_t \geq 0$ and $W_t \geq 0$, we have

$$K\left[\phi_t W_t \left(\frac{p_{t+dt} - p_t}{p_t} - \bar{r}\, dt\right)\right] = \phi_t W_t \cdot K\left(\frac{p_{t+dt} - p_t}{p_t} - \bar{r}\, dt\right).$$

From Lemma 1 we then get

$$\begin{aligned}
&\lim_{dt\to 0} \frac{1}{dt} K\left(\frac{p_{t+dt} - p_t}{p_t} - \bar{r}\, dt\right) \\
&= \lim_{dt\to 0} \frac{1}{dt} \int_t^{t+dt} \mathcal{D}^+ K\left[\frac{p_s - p_t}{p_t} - \bar{r}(s-t)\right] d\left[\frac{p_s - p_t}{p_t} - \bar{r}(s-t)\right] \\
&\qquad + \frac{1+\kappa}{2} \lim_{\epsilon\to 0} \frac{1}{2\epsilon} \lim_{dt\to 0} \frac{1}{dt} \int_t^{t+dt} 1_{(-\epsilon,\,\epsilon)}\left[\frac{p_s - p_t}{p_t} - \bar{r}(s-t)\right] ds \\
&= \left[1_{[0,\infty)}\left(\frac{dp_t}{p_t} - \bar{r}\, dt\right) - \kappa \cdot 1_{(-\infty,0)}\left(\frac{dp_t}{p_t} - \bar{r}\, dt\right)\right] (\mu_t^p - \bar{r}) \\
&\quad + \lim_{dt\to 0} \frac{1}{dt} \int_t^{t+dt} \mathcal{D}^+ K\left[\frac{p_s - p_t}{p_t} - \bar{r}(s-t)\right] \left(\sigma_{1t}^p\, dB_{1s} + \sigma_{2t}^p\, dB_{2s}\right) \\
&\quad + \frac{1+\kappa}{2} \cdot 1_{\{0\}}\left(\frac{dp_t}{p_t} - \bar{r}\, dt\right).
\end{aligned}$$

Consequently,

$$\begin{aligned}
&\lim_{dt\to 0} \mathrm{E}_t\left[\frac{1}{dt} K\left(\frac{p_{t+dt} - p_t}{p_t} - \bar{r}\, dt\right)\right] \\
&= \mathrm{E}_t\left[\lim_{dt\to 0} \frac{1}{dt} K\left(\frac{p_{t+dt} - p_t}{p_t} - \bar{r}\, dt\right)\right] \\
&= \mathrm{E}_t\left[1_{[0,\infty)}\left(\frac{dp_t}{p_t} - \bar{r}\, dt\right) - \kappa \cdot 1_{(-\infty,0)}\left(\frac{dp_t}{p_t} - \bar{r}\, dt\right)\right] \cdot (\mu_t^p - \bar{r}) \\
&\qquad + \lim_{dt\to 0} \frac{1}{dt} \mathrm{E}_t\left\{\int_t^{t+dt} \mathcal{D}^+ K\left[\frac{p_s - p_t}{p_t} - \bar{r}(s-t)\right] \left(\sigma_{1t}^p\, dB_{1s} + \sigma_{2t}^p\, dB_{2s}\right)\right\} \\
&\qquad + \frac{1+\kappa}{2} \mathrm{E}_t\left[1_{\{0\}}\left(\frac{dp_t}{p_t} - \bar{r}\, dt\right)\right] \\
&= \left[P_t\left(\frac{dp_t}{p_t} - \bar{r}\, dt \geq 0\right) - \kappa \cdot P_t\left(\frac{dp_t}{p_t} - \bar{r}\, dt < 0\right)\right] (\mu_t^p - \bar{r}) \\
&\qquad + 0 + \frac{1+\kappa}{2} P_t\left(\frac{dp_t}{p_t} = \bar{r}\, dt\right) \\
&= \left[P_t\left(\frac{dp_t}{p_t} \geq \bar{r}\, dt\right) - \kappa \cdot P_t\left(\frac{dp_t}{p_t} < \bar{r}\, dt\right)\right] (\mu_t^p - \bar{r}).
\end{aligned}$$

QED.

Appendix 2: The Derivation of (25)

For the given time interval $[0,\ T]$, we adopt Duan's (1997) approach to express (24) as the following lattice process:

$$\Delta y_{k/n} \equiv r_{k/n} = (\delta_\circ + \delta_1 h_{k/n})\cdot n^{-1} + (1+2\eta\lambda)\sqrt{h_{k/n}}\cdot v_k \cdot n^{-1/2} - \lambda h_{k/n}(v_k^2 - 1)n^{-1/2},$$

for $(k-1)/n \le t < k/n$. Here $y_{k/n}$ denotes the log stock price at time k/n such that $r_{k/n} = y_{k/n} - y_{(k-1)/n} \equiv \Delta y_{k/n}$. Note that the drift is made of order n^{-1} whereas the diffusion is of order $n^{-1/2}$. Similarly, (20) can be expressed as:

$$\Delta h_{k/n} \equiv h_{k/n} - h_{(k-1)/n} = \left[(\omega + \alpha\eta^2) - (1-\alpha-\beta)h_{(k-1)/n}\right]\cdot n^{-1}$$
$$- 2\alpha\eta\sqrt{h_{(k-1)/n}}\cdot v_k \cdot n^{-1/2} + \alpha h_{(k-1)/n}(v_k^2 - 1)\cdot n^{-1/2}.$$

If the first two moments of $\Delta y_{k/n}$ and $\Delta h_{k/n}$ converge to well-behaved limits, and moments with orders higher than two are all converge to zero, then Nelson (1990, 1992) and Nelson and Foster's (1994) theory of continuous record asymptotics ensure that $\Delta y_{k/n}$ and $\Delta h_{k/n}$ will converge to a bivariate diffusion process. Hence, we will check each of the first two moments of $\Delta y_{k/n}$ and $\Delta h_{k/n}$ to see whether it converges. As $n \to \infty$, we have

$$n\cdot \mathrm{E}_{(k-1)/n}(\Delta y_{k/n}) = \delta_\circ + \delta_1 h_{k/n} \longrightarrow \delta_\circ + \delta_1 h_t,$$

$$n\cdot \mathrm{E}_{(k-1)/n}(\Delta h_{k/n}) = (\omega + \alpha\eta^2) - (1-\alpha-\beta)h_{(k-1)/n} \longrightarrow (\omega + \alpha\eta^2) - (1-\alpha-\beta)h_t,$$

$$n\cdot \mathrm{E}_{(k-1)/n}[(\Delta y_{k/n})^2] = (1+2\eta\lambda)^2 h_{k/n} + 2\lambda^2 h_{k/n}^2 \longrightarrow (1+2\eta\lambda)^2 h_t + 2\lambda^2 h_t^2,$$

$$n\cdot \mathrm{E}_{(k-1)/n}\left[(\Delta h_{k/n})^2\right] = 4\alpha^2\eta^2 h_{(k-1)/n} + 2\alpha^2 h_{(k-1)/n} \longrightarrow 4\alpha^2\eta^2 h_t + 2\alpha^2 h_t,$$

and

$$n\cdot \mathrm{E}_{(k-1)/n}[(\Delta y_{k/n})(\Delta h_{k/n})] = -2\alpha(1+2\eta\lambda)\eta\sqrt{h_{k/n}\cdot h_{(k-1)/n}} - 2\alpha\lambda h_{k/n}\cdot h_{(k-1)/n}$$
$$\longrightarrow -2\alpha(1+2\eta\lambda)\eta h_t - 2\alpha\lambda h_t^2.$$

It is readily seen that moments with orders higher than two are all converge to zero. Given these results, the existence of (25) is guaranteed.

References

Ait-Sahalia, Y., 1996, "Nonparametric Pricing of Interest Rate Derivative Securities," *Econometrica*, 64, 527–560.

Andersen, T., L. Benzoni and J. Lund, 2002, "An Empirical Investigation of Continuous-Time Models for Equity Returns," *Journal of Finance*, 57, 1239-1284.

Andersen, T., and J., Lund, 1997, "Estimating Continuous Time Stochastic Volatility Models of the Short Term Interest Rate," *Journal of Econometrics*, 77, 343–378.

Barberis, N., and M. Huang, 2001, "Mental Accounting, Loss Aversion and Individual Stock Returns", *Journal of Finance*, 56, 1247–1292.

Barberis, N., and M. Huang, 2003, "Preferences with Frames: A New Utility Specification that Allows for the Framing of Risks", *Working Paper*, University of Chicago.

Barberis, N., and M. Huang, 2004, "The Loss Aversion / Narrow Framing Approach to Stock Market Pricing and Participation Puzzles", prepared for the *Handbook of Investments: Equity Risk Premium*, R. Mehra ed., North Holland, Amsterdam.

Barberis, N., M. Huang and T. Santos, 2001, "Prospect Theory and Asset Prices", *Quarterly Journal of Economics*, 116, 1–53.

Barberis, N., M. Huang and R. Thaler, 2003, "Individual Preferences, Montary Gambles and Equity Premium", *Working Paper*, University of Chicago.

Barberis, N., and R. Thaler, 2003, "A Survey of Behavior Finance", , in *Handbook of the Economics and Finance*, George Constantinides, Milton Harris, and Rene Stulz eds., North-Holland.

Benartzi, S., and R. Thaler, 1995, "Myopic Loss Aversion and the Equity Premium Puzzle", *Quarterly Journal of Economics*, 52, 75–92.

Bekaert, G., and G. Wu., 2000, "Asymmetric Volatility and Risk in Equity Market," *Review of Financial Studies*, 13, 1–42.

Berkelaar, A., R. Kouwenberg, and T. Post, 2004, "Optimal Portfolio Choice under Loss Aversion," forthcoming, *Review of Economics and Statistics*.

Brennan, M. J., E. S. Schwartz, and R. Lagnado, 1997, "Strategic Asset Allocation," *Journal of Economic Dynamics and Control*, 21, 1377–1403.

Campbell, J. Y., 1991, "A Variance Decomposition for Stock Returns," *Economic Journal*, 101, 157–179.

Campbell, J. Y., and L. Hentschel, 1992, "No News is Good News. An Asymmetric Model of Changing Volatility in Stock Return," *Journal of Financial Economics*, 31, 281–318.

Campbell, J. Y., and R., Shiller, 1988, "The Dividend-Price Ratio and Expectation of Future Dividends and Discount Factors," *Review of Financial Studies*, 1, 195–227.

Chernov, M., and E., Ghysels, 2000, "A Study Towards a Unified Approach to the Joint Estimation of Objective and Risk Neutral Measures for the Purpose of Options Valuation," *Journal of Financial Economics*, 56, 407–458.

Chernov, M., A. R. Gallant, E. Ghysels and G. Tauchen, 2003, "Alternative Models for Stock Price Dynamics," *Journal of Econometrics*, 116, 225–258.

Chung, K. L., and R. Williams, 1990, *An Introduction to Stochastic Integration,* 2nd ed. Boston: Birkhäuser.

Dai, Q., and J. Singleton, 2001, “Specification Analysis of Affine Term Structure Models,” *Journal of Finance*, 55, 1943–1978.

Das, S. R., and R. Uppal, 2004, “Systemic Risk and International Portfolio Choice,” *Journal of Finance*, 59, 2809–2834.

Duan, J.-C., 1997, “Augmented GARCH (p,q) Process and its Diffusion Limit,” *Journal of Econometrics*, 79, 97–127.

Duffie, Da., J. Pan, and K. Singleton, 2000, “Transform Analysis and Asset Pricing for Affine Jump Diffusion,” *Econometrica*, 68, 1343–1376.

Duffie, D., and K. J. Singleton, 1993, “Simulated Moments Estimation of Markov Models of Asset Prices”, *Econometrica*, 61, 929–952.

Elerian, O., S. Chib and N. Shephard, 2001, “Likelihood Inference for Discretely Observed Nonlinear Diffusions”, *Econometrica*, 69, 959–994.

Eraker, B., 2001, “MCMC Analysis of Diffusion Models with Application to Finance”, *Journal of Business and Economic Statistics*, 19, 177–191.

Eraker, B., 2004, “Do stock prices and volatility jump? Reconciling evidence from spot and option prices”, *Journal of Finance*, 59, 1367–1403.

Gallant, A. R., and Tauchen, G., 1996, “Which Moments to Match?,” *Econometric Theory*, 12, 657–681.

Gallant, A. R., and G. Tauchen, 2002, “Simulated Score Methods and Indirect Inference for Continuous-time Models,” *prepared for the Handbook of Financial Econometrics*, available at http://www.econ.duke.edu/ get/wpapers

Gomes, F., 2005, “Portfolio Choice and Trading Volume with Loss Averse Investors,” forthcoming, *Journal of Business*.

Hansen, L. P., and J. A. Scheinkman, 1995, “Back to the Future: Generating Moment Implication for Continuous-Time Markov Process,” *Econometrica*, 63, 767–804.

Heston, S. L., 1993, “A Closed Form Solution for Options with Stochastic Volatility with Applications to Bond and Currency Options”, *Review of Financial Studies*, 6, 327–389.

Kahneman, D., and D. Lovallo, 1993, “Timid Choices and Bold Forecasts: A Cognitive Perspective on Risk Taking,” *Management Science*, 39, 17–31.

Kahneman, D., and A. Tversky, 1979, “Prospect Theory: An Analysis of Decision under Risk”, *Econometirca*, 47, 263–291.

Klebaner, F., 1998, *Introduction to Stochastic Calculus with Application*, Imperial College Press.

Liu, J., 2001, “Portfolio Selection in Stochastic Environments,” Unpublished Working Paper, University of California at Los Angeles.

Liu, J., F. Longstaff, and J. Pan, 2003, “Dynamic Asset Allocation with Event Risk,” *Journal of Finance*, 58, 231–259.

Maenhout, P., 2001, “Robust Portfolio Rules and Asset Pricing”, *Working Paper*, Harvard University.

Mankiw, N., and S. Zeldes, 1991, “The Consumption of Stockholders and Non-stockholders,” *Journal of Financial Economics*, 29, 97–112.

Mehra R., and E. C. Prescott, 2003, “The Equity Premium in Retrospect,” in *Handbook of the Economics of Finance*, Ed. by G.M. Constantinides, M. Harris and R. Stulz, Elsevier B.V.

Nelson, D. B., 1990, “ARCH Models As Diffusion Approximation,” *Journal of Econometrics*, 45, 7–38.

Nelson, D. B., 1992, “Filtering and Forecasting with Misspecification ARCH Models I: Getting the Right Variance with the Wrong Model,” *Journal of Econometrics*, 52, 61–90.

Nelson, D. B. and D. P. Foster, 1994, “Asymptotic Filtering Theory for Univariate ARCH Models,” *Econometrica*, 62, 1–41.

Read, D., G. Loewenstein, and M. Rabin, 1999, “Choice Bracketing,” *Journal of Risk and Uncertainty*, 19, 171–197.

Shumway, T., 1997, “Explaining Returns with Loss Aversion,” *Working Paper*, University of Michigan.

Thaler, R., 1980, “Toward A Positive Theory of Consumer Choice,” *Journal of Economic Behavior and Organization*, 1, 39–60.

Thaler, R., A. Tversky, D. Kahneman and A. Schwartz, 1997, “The Effect of Myopic and Loss Aversion on Risk-Taking: An Experiment Test”, *Quarterly Journal of Economics*, 112, 643–660.

Tversky, A., and D. Kahneman, 1991, “Loss Aversion in Riskless Choice: A Reference-Dependent Model,” *Quarterly Journal of Economics*, 106, 1039–1061.

Tversky, A., and D. Kahneman, 1992, “Advances in Prospect Theory: Cumulative Representation of Uncertainty,” *Journal of Risk and Uncertainty*, 5, 297–323.

Uppal, R., and T. Wang, 2003, “Model Misspecification and Under Diversification”, *Journal of Finance*, 58, 2465–2486.

Van der Sluis, P. J., 1997, “EmmPack 1.01: C/C++ Code for Use with Ox for Estimation of Univariate Stochastic Volatility Models with the Efficient Method of Moments,” *Nonlinear Dynamics and Econometrics*, 2, 77–94.

Wu, G., 2001, “The Determinants of Asymmetric Volatility,” *Review of Financial Studies*, 14, 837–859

Xia, Y., 2001, “Learning About Predictability: The Effects of Parameter Uncertainty on Dynamic Asset Allocation,” *Journal of Finance*, 56, 205–246.